

# Fermionic condensate and Casimir densities in the presence of compact dimensions with applications to nanotubes

E. Elizalde<sup>1</sup>, S. D. Odintsov<sup>1,2\*</sup>, A. A. Saharian<sup>3</sup>

<sup>1</sup>*Instituto de Ciencias del Espacio (CSIC)  
and Institut d'Estudis Espacials de Catalunya (IEEC/CSIC)  
Campus UAB, Facultat de Ciències, Torre C5-Parell-2a planta,  
08193 Bellaterra (Barcelona) Spain*

<sup>2</sup>*Institució Catalana de Recerca i Estudis Avançats (ICREA)*

<sup>3</sup>*Department of Physics, Yerevan State University,  
1 Alex Manoogian Street, 0025 Yerevan, Armenia*

February 16, 2022

## Abstract

We investigate the fermionic condensate and the vacuum expectation value of the energy-momentum tensor for a massive fermionic field in the geometry of two parallel plates on the background of Minkowski spacetime with an arbitrary number of toroidally compactified spatial dimensions, in the presence of a constant gauge field. Bag boundary conditions are imposed on the plates and periodicity conditions with arbitrary phases are considered along the compact dimensions. The nontrivial topology of the background spacetime leads to an Aharonov-Bohm effect for the vacuum expectation values induced by the gauge field. The fermionic condensate and the expectation value of the energy-momentum tensor are periodic functions of the magnetic flux with period equal to the flux quantum. The boundary induced parts in the fermionic condensate and the vacuum energy density are negative, with independence of the phases in the periodicity conditions and of the value of the gauge potential. Interaction forces between the plates are thus always attractive.

However, in physical situations where the quantum field is confined to the region between the plates, the pure topological part contributes as well, and then the resulting force can be either attractive or repulsive, depending on the specific phases encoded in the periodicity conditions along the compact dimensions, and on the gauge potential, too. Applications of the general formulas to cylindrical carbon nanotubes are considered, within the framework of a Dirac-like theory for the electronic states in graphene. In the absence of a magnetic flux, the energy density for semiconducting nanotubes is always negative. For metallic nanotubes the energy density is positive for long tubes and negative for short ones. The resulting Casimir forces acting on the edges of the nanotube are attractive for short tubes with independence of the tube chirality. The sign of the force for long nanotubes can be controlled by tuning the magnetic flux. This opens the way to the design of efficient actuators driven by the Casimir force at the nanoscale.

---

\*Also at Tomsk State Pedagogical University, Tomsk

# 1 Introduction

In a good number of problems one needs to consider a physical model on the background of some manifold with compactified spatial dimensions. Many high-energy theories of fundamental physics are formulated in a higher dimensional spacetime and it is commonly assumed that the extra dimensions are compactified. In particular, additional compact dimensions have been extensively used in supergravity and superstring theories. From the inflationary point of view, universes with compact dimensions, under certain conditions, should be considered a rule rather than an exception [1]. Models of a compact universe with non-trivial topology may play an important role by providing proper initial conditions for inflation. There has been a large activity to search for signatures of non-trivial topology by identifying ghost images of galaxies, clusters or quasars. Recent progress in observations of the cosmic microwave background provides an alternative way to observe the topology of the universe. An interesting application of the field theoretical models with compact dimensions recently appeared in nanophysics [2]. The long-wavelength description of the electronic states in graphene can be formulated in terms of the Dirac-like theory in 3-dimensional spacetime with the Fermi velocity playing the role of speed of light (see, e.g., Refs. [3, 4]). Single-walled carbon nanotubes are generated by rolling up a graphene sheet to form a cylinder and the background spacetime for the corresponding Dirac-like theory has topology  $R^2 \times S^1$ . For another class of graphene-made structures, called toroidal carbon nanotubes, one has as background topology  $R^1 \times (S^1)^2$ .

The boundary conditions imposed on fields along compact dimensions give rise to a modification of the spectrum of the vacuum fluctuations and, as a result, to Casimir-type contributions in the vacuum expectation values of physical observables (for the topological Casimir effect and its role in cosmology see [5] and references therein). In models of Kaluza-Klein type, the Casimir effect has been used as a stabilization mechanism for moduli fields and as a source for dynamical compactification of the extra dimensions, in particular, for quantum Kaluza-Klein gravity (see Ref. [6]). The Casimir energy can also serve as a model for dark energy needed for the explanation of the present accelerated expansion of the universe (see [7] and references therein). In addition, recent measurements of the Casimir forces between macroscopic bodies provide a sensitive test for constraining the parameters of long-range interactions, as predicted by modern unification theories of fundamental interactions [8]. The influence of extra compactified dimensions on the Casimir effect in the classical configuration of two parallel plates has been recently discussed in [9], for the case of a scalar field, and in [10], for the electromagnetic field with perfectly conducting boundary conditions.

More recently, interest has been focussed on the topic of the Casimir effect in braneworld models with large extra dimensions. This type of models (for a review see [11]) naturally appear in the string/M theory context and they provide a novel set up for discussing phenomenological and cosmological issues related with extra dimensions. In braneworld models the investigation of quantum effects is of considerable phenomenological value, both in particle physics and in cosmology. The braneworld corresponds to a manifold with boundaries and the bulk fields will give Casimir-type contributions to the vacuum energy and, as a result, to the vacuum forces acting on the branes. The Casimir forces provide a natural mechanism for stabilizing the radion field in the Randall-Sundrum model, as required for a complete solution of the hierarchy problem. In addition, the Casimir energy gives a contribution to both the brane and the bulk cosmological constants. Hence, it has to be taken into account in any self-consistent formulation of the braneworld dynamics. The Casimir energy and corresponding Casimir forces within the framework of the Randall-Sundrum braneworld [12] have been evaluated in Refs. [13] by using both dimensional and zeta function regularization methods. Local Casimir densities were considered in Ref. [14]. The Casimir effect in higher dimensional generalizations of the

Randall-Sundrum model with compact internal spaces has been investigated in [15].

In the present paper we will study the fermionic condensate, the Casimir energy density and the vacuum stresses for a massive fermion field in the geometry of two parallel plates on a spacetime with an arbitrary number of toroidally compactified spatial dimensions. We will impose generalized periodicity conditions along the compact dimensions with arbitrary phases and MIT bag boundary conditions on the plates. The presence of a constant gauge field will be assumed as well. Though the corresponding field strength vanishes, the nontrivial topology of the background spacetime leads to Aharonov-Bohm-like effects on the vacuum expectation values. The total Casimir energy in the geometry under consideration has been discussed in Ref. [16], in the absence of a gauge field. The investigation of local physical characteristics in the Casimir effect, such as the expectation value of the energy-momentum tensor and the fermionic condensate, is of considerable interest. Indeed, local quantities contain more information on the vacuum fluctuations than global ones. In addition to describing the physical structure of the quantum field at a given point, the energy-momentum tensor acts as the source in Einstein's equations and, therefore, it plays an important role in modeling a self-consistent dynamics which involves the gravitational field. The fermionic condensate plays an important role in the models of dynamical chiral symmetry breaking (see review [17] for chiral symmetry breaking in the Nambu-Jona-Lasino and Gross-Neveu models on the background of a curved spacetime with non-trivial topology and [18] for very recent developments).

The fermion Casimir energy for two parallel plates in 4-dimensional Minkowski spacetime with trivial topology has been considered in [19], for a massless field, and in [20] in the massive case. For arbitrary number of dimensions, the corresponding results are generalized in Refs. [21, 22] for the massless and massive cases, respectively. The fermionic condensate for a massless field has been considered in Refs. [23]. The Casimir problem for fermions coupled to a static background field in one spatial dimension is investigated in [24]. The interaction energy density and the corresponding force are computed in the limit that the background becomes concentrated at two points. The fermionic Casimir effect for parallel plates with imperfect bag boundary conditions modelled by  $\delta$ -like potentials is studied in [25]. The topological Casimir effect and the vacuum expectation value of the fermionic current for a massive fermionic field in a spacetime with an arbitrary number of toroidally compactified spatial dimensions have been considered in [26, 27].

The paper is organized as follows. In the next section, we specify the eigenfunctions and the eigenmodes for the Dirac equation in the region between the plates assuming bag boundary conditions on them. The fermionic condensate in this region is considered in Sect. 3. By using an Abel-Plana-type summation formula, we express the condensate as the sum of a pure topological, single plate contribution and interference parts. Various limiting cases are then considered. The vacuum expectation value of the energy-momentum tensor is investigated in Sect. 4. A generalization for a conformally-flat background spacetime is given. In Sect. 5 we study applications of the general formulas to the Casimir effect for electrons in a carbon nanotube, within the framework of a 3-dimensional Dirac-like model. The main results of the paper are summarized in Sect. 6.

## 2 Fermionic eigenfunctions

Consider a spinor field,  $\psi$ , propagating on a  $(D + 1)$ -dimensional flat spacetime with spatial topology  $R^{p+1} \times (S^1)^q$ ,  $p + q + 1 = D$ . We will denote by  $\mathbf{z}_{p+1} = (z_1, \dots, z_{p+1} \equiv z)$  and  $\mathbf{z}_q = (z_{p+2}, \dots, z_D)$  the Cartesian coordinates along the uncompactified and the compactified dimensions, respectively. For these coordinates we have  $-\infty < z_l < \infty$ ,  $l = 1, \dots, p + 1$ , and  $0 \leq z_l \leq L_l$  for  $l = p + 2, \dots, D$ , with  $L_l$  being the length of the  $l$ -th compact dimension. We

assume that along the compactified dimensions the field obeys quasiperiodic boundary conditions

$$\psi(t, \mathbf{z}_{p+1}, \mathbf{z}_q + L_l \mathbf{e}_l) = e^{2\pi i \alpha_l} \psi(t, \mathbf{z}_{p+1}, \mathbf{z}_q), \quad (2.1)$$

with constant phases  $|\alpha_l| \leq 1/2$  and  $\mathbf{e}_l$  is the unit vector along the direction of the coordinate  $z_l$ ,  $l = p+2, \dots, D$ . Condition (2.1) includes the periodicity conditions for both untwisted and twisted fermionic fields as special cases with  $\alpha_l = 0$  and  $\alpha_l = 1/2$ , respectively. The special cases  $\alpha_l = 0, \pm 1/3$  are realized in nanotubes.

In this paper we are interested in the fermionic condensate and in the vacuum expectation value (VEV) of the energy-momentum tensor induced by two parallel plates located at  $z = 0$  and  $z = a$ . On the boundaries the field obeys MIT bag boundary conditions

$$(1 + i\gamma^\mu n_\mu) \psi = 0, \quad z = 0, a, \quad (2.2)$$

with  $\gamma^\mu$  being the Dirac matrices and  $n_\mu$  the outward oriented (with respect to the region under consideration) normal to the boundary. Note that from the conditions (2.2) it follows that, on the boundaries,  $\bar{\psi}\psi = 0$  and  $n_\mu \bar{\psi} \gamma^\mu \psi = 0$ , where  $\bar{\psi} = \psi^\dagger \gamma^0$  is the Dirac adjoint and the dagger denotes Hermitian conjugation. In the discussion below the calculations will be done for the region between the plates,  $0 < z < a$ , where we have  $n_\mu = -\delta_\mu^{p+1}$  at  $z = 0$  and  $n_\mu = \delta_\mu^{p+1}$  at  $z = a$ . The expressions for the VEVs in the regions  $z < 0$  and  $z > a$  are obtained as limiting cases.

Dynamics of the massive spinor field is governed by the Dirac equation

$$i\gamma^\mu \partial_\mu \psi - m\psi = 0. \quad (2.3)$$

In the  $(D+1)$ -dimensional spacetime, the Dirac matrices are  $N_D \times N_D$  matrices with  $N_D = 2^{\lfloor (D+1)/2 \rfloor}$ , where the square brackets mean integer part of the enclosed expression. We will take these matrices in the Dirac representation:

$$\gamma^0 = \begin{pmatrix} 1 & 0 \\ 0 & -1 \end{pmatrix}, \quad \gamma^\mu = \begin{pmatrix} 0 & \sigma_\mu^+ \\ -\sigma_\mu^+ & 0 \end{pmatrix}, \quad \mu = 1, 2, \dots, D. \quad (2.4)$$

From the anticommutation relations for the Dirac matrices one has  $\sigma_\mu \sigma_\nu^+ + \sigma_\nu \sigma_\mu^+ = 2\delta_{\mu\nu}$ . In the case  $D = 2$  we have  $N_D = 2$  and the Dirac matrices are  $\gamma^\mu = (\sigma_{P3}, i\sigma_{P1}, i\sigma_{P2})$ , with  $\sigma_{P\mu}$  being the  $2 \times 2$  Pauli matrices.

The boundary conditions (2.1) and (2.2) lead to the modification of the spectrum for vacuum fluctuations of the fermionic field and, as a result, to the topological and boundary induced Casimir effects on the VEVs of physical observables. For the evaluation of the VEVs we need the complete set of positive- and negative-energy solutions to the Dirac equation satisfying the boundary conditions (2.2). The dependence on the coordinates parallel to the plates,  $\mathbf{z}_\parallel = (z_1, \dots, z_p, z_{p+2}, \dots, z_D)$ , can be presented in the standard exponential form  $\exp(i\mathbf{k}_\parallel \cdot \mathbf{z}_\parallel)$ , with  $\mathbf{k}_\parallel = (\mathbf{k}_p, \mathbf{k}_q)$  and  $\mathbf{k}_p = (k_1, \dots, k_p)$ ,  $\mathbf{k}_q = (k_{p+2}, \dots, k_D)$ . The eigenvalues for the components of the wave vector along the compactified dimensions are determined from the periodicity conditions (2.1):

$$\mathbf{k}_q = (2\pi(n_{p+2} + \alpha_{p+2})/L_{p+2}, \dots, 2\pi(n_D + \alpha_D)/L_D), \quad (2.5)$$

with  $n_{p+2}, \dots, n_D = 0, \pm 1, \pm 2, \dots$ . For the components along the uncompactified dimensions one has  $-\infty < k_l < \infty$ ,  $l = 1, \dots, p$ . The corresponding positive- and negative-energy eigenspinors have the form

$$\begin{aligned} \psi_\beta^{(+)} &= A_\beta e^{-i\omega t} \begin{pmatrix} \varphi \\ -i\boldsymbol{\sigma}^+ \cdot \nabla \varphi / (\omega + m) \end{pmatrix}, \\ \psi_\beta^{(-)} &= A_\beta e^{i\omega t} \begin{pmatrix} i\boldsymbol{\sigma} \cdot \nabla \chi / (\omega + m) \\ \chi \end{pmatrix}, \end{aligned} \quad (2.6)$$

where  $\boldsymbol{\sigma} = (\sigma_1, \dots, \sigma_D)$ ,  $\omega = \sqrt{\mathbf{k}_p^2 + k_{p+1}^2 + \mathbf{k}_q^2 + m^2}$  and  $\beta$  is the collective index for the set of quantum numbers specifying the solutions (see below). The spinors in (2.6) are given by the expressions

$$\begin{aligned}\varphi &= e^{i\mathbf{k}_{\parallel} \cdot \mathbf{z}_{\parallel}} \left( \varphi_+ e^{ik_{p+1}z} + \varphi_- e^{-ik_{p+1}z} \right), \\ \chi &= e^{-i\mathbf{k}_{\parallel} \cdot \mathbf{z}_{\parallel}} \left( \chi_+ e^{ik_{p+1}z} + \chi_- e^{-ik_{p+1}z} \right),\end{aligned}\quad (2.7)$$

From the boundary condition (2.2) on the plate at  $z = 0$  we find the following relations between the spinors in (2.7)

$$\begin{aligned}\varphi_+ &= -\frac{m(\omega + m) + k_{p+1}^2 - k_{p+1}\sigma_{p+1}\boldsymbol{\sigma}_{\parallel}^+ \cdot \mathbf{k}_{\parallel}}{(m - ik_{p+1})(\omega + m)}\varphi_-, \\ \chi_- &= -\frac{m(\omega + m) + k_{p+1}^2 - k_{p+1}\sigma_{p+1}\boldsymbol{\sigma}_{\parallel}^+ \cdot \mathbf{k}_{\parallel}}{(m + ik_{p+1})(\omega + m)}\chi_+, \end{aligned}\quad (2.8)$$

where  $\boldsymbol{\sigma}_{\parallel} = (\sigma_1, \dots, \sigma_p, \sigma_{p+2}, \dots, \sigma_D)$ . We will assume that they are normalized in accordance with  $\varphi_-^+ \varphi_- = \chi_+^+ \chi_+ = 1$ . As a set of independent spinors we will take  $\varphi_- = w^{(\sigma)}$  and  $\chi_+ = w^{(\sigma)'}$ , where  $w^{(\sigma)}$ ,  $\sigma = 1, \dots, N_D/2$ , are one-column matrices having  $N_D/2$  rows with the elements  $w_i^{(\sigma)} = \delta_{i\sigma}$ , and  $w^{(\sigma)'} = iw^{(\sigma)}$ . Now the set of quantum numbers specifying the eigenfunctions (2.6) is  $\beta = (\mathbf{k}, \sigma)$ . From the boundary condition at  $z^{p+1} = a$  it follows that the eigenvalues of  $k_{p+1}$  are roots of the transcendental equation

$$ma \sin(k_{p+1}a)/(k_{p+1}a) + \cos(k_{p+1}a) = 0. \quad (2.9)$$

All these roots are real. We will denote the positive solutions of Eq. (2.9) by  $\lambda_n = k_{p+1}a$ ,  $n = 1, 2, \dots$ . For a massless field one has  $\lambda_n = \pi(n - 1/2)$ . Note that Eq. (2.9) does not contain the parameters of the compact subspace and is the same as in the corresponding problem on the topologically trivial Minkowski spacetime (see [5]). Note that this will not be the case in a more general class of compact subspaces.

The normalization coefficient  $A_{\beta}$  in (2.6) is determined from the orthonormalization condition

$$\int d\mathbf{z}_{\parallel} \int_0^a dz^{p+1} \psi_{\beta}^{(\pm)+} \psi_{\beta'}^{(\pm)-} = \delta_{\beta\beta'}. \quad (2.10)$$

Here, the symbol  $\delta_{\beta\beta'}$  is understood as the Dirac delta function for continuous indices and the Kronecker delta for discrete ones. The substitution of the eigenfunctions (2.6) into this condition leads to the result

$$A_{\beta}^2 = \frac{\omega + m}{4(2\pi)^p \omega a V_q} \left[ 1 - \frac{\sin(2k_{p+1}a)}{2k_{p+1}a} \right]^{-1}, \quad (2.11)$$

where  $V_q = L_{p+2} \cdots L_D$  is the volume of the compact subspace.

We can generalize the eigenfunctions given above to the situation when an external electromagnetic field with vector potential  $A_{\mu} = \text{const}$  is present. In spite of the fact that the corresponding magnetic field strength vanishes, the non-trivial topology of the background spacetime leads to the appearance of an Aharonov-Bohm-like effect for the physical observables. In particular, the corresponding VEVs depend on  $A_{\mu}$ . Now the Dirac equation has the form  $i\gamma^{\mu}(\partial_{\mu} + ieA_{\mu})\psi - m\psi = 0$  and, by making use the gauge transformation  $A_{\mu} = A'_{\mu} + \partial_{\mu}\Lambda(x)$ ,  $\psi(x) = \psi'(x)e^{-ie\Lambda(x)}$ , with the function  $\Lambda(x) = A_{\mu}x^{\mu}$ , we see that the new function  $\psi'(x)$  satisfies the Dirac equation with  $A'_{\mu} = 0$  and the quasiperiodicity conditions similar to (2.1) with the replacement

$$\alpha_l \rightarrow \tilde{\alpha}_l = \alpha_l + eA_l L_l / (2\pi). \quad (2.12)$$

The eigenvalues for the wave vector components along compact dimensions are defined by  $k_l = 2\pi(n_l + \tilde{\alpha}_l)/L_l$  and the corresponding eigenspinors are obtained from those given above with the replacement (2.12).

### 3 Fermionic condensate

The fermionic condensate is among the most important quantities that characterize the properties of the quantum vacuum. Although the corresponding operator is local, due to the global nature of the vacuum, this quantity carries important information about the global properties of the background spacetime. Having the complete set of eigenspinors, we can evaluate the fermionic condensate by using the mode-sum

$$\langle \bar{\psi}\psi \rangle = \sum_{\beta} \bar{\psi}_{\beta}^{(-)}(x)\psi_{\beta}^{(-)}(x), \quad (3.1)$$

where  $\langle \dots \rangle$  stands for VEV. By taking into account the expression (2.6) for the negative-energy eigenspinors, the fermionic condensate in the region between the plates can be expressed as

$$\begin{aligned} \langle \bar{\psi}\psi \rangle &= -\frac{N_D}{aV_q} \sum_{\mathbf{n}_q \in \mathbf{Z}^q} \int \frac{d\mathbf{k}_p}{(2\pi)^p} \sum_{n=1}^{\infty} \frac{\sin(\lambda_n z/a)}{\omega a} \\ &\times \frac{ma \sin(\lambda_n z/a) + \lambda_n \cos(\lambda_n z/a)}{1 - \sin(2\lambda_n)/(2\lambda_n)}, \end{aligned} \quad (3.2)$$

where  $\mathbf{n}_q = (n_{p+2}, \dots, n_D)$  and

$$\omega = \sqrt{\lambda_n^2/a^2 + \mathbf{k}_p^2 + \mathbf{k}_q^2 + m^2}. \quad (3.3)$$

Of course, the expression on the rhs of Eq. (3.2) is divergent. We will assume that some cutoff function is present, without writing it explicitly.

For the further evaluation of the fermionic condensate we apply to the sum over  $n$  in Eq. (3.2) the Abel-Plana-type summation formula

$$\sum_{n=1}^{\infty} \frac{\pi f(\lambda_n)}{1 - \sin(2\lambda_n)/(2\lambda_n)} = -\frac{\pi m a f(0)}{2(ma + 1)} + \int_0^{\infty} dx f(x) - i \int_0^{\infty} dx \frac{f(ix) - f(-ix)}{\frac{x+ma}{x-ma} e^{2x} + 1}, \quad (3.4)$$

with the function

$$f(x) = \frac{\sin(xz/a)}{\sqrt{x^2 + \mathbf{k}_p^2 a^2 + m_{\mathbf{n}_q}^2 a^2}} [ma \sin(xz/a) + x \cos(xz/a)]. \quad (3.5)$$

Formula (3.4) is a special case of the summation formula derived in Ref. [29] on the basis of the generalized Abel-Plana formula (see also Ref. [30]). In Eq. (3.5) and the discussion below we use the notation

$$m_{\mathbf{n}_q}^2 = k_{\mathbf{n}_q}^2 + m^2, \quad k_{\mathbf{n}_q}^2 = \sum_{l=p+2}^D [2\pi(n_l + \alpha_l)/L_l]^2. \quad (3.6)$$

After the application of formula (3.4), the fermionic condensate is split into

$$\begin{aligned} \langle \bar{\psi}\psi \rangle &= \langle \bar{\psi}\psi \rangle^{(0)} + \langle \bar{\psi}\psi \rangle^{(1)} - \frac{2N_D}{\pi V_q} \sum_{\mathbf{n}_q \in \mathbf{Z}^q} \int \frac{d\mathbf{k}_p}{(2\pi)^p} \int_{\sqrt{\mathbf{k}_p^2 + m_{\mathbf{n}_q}^2}}^{\infty} dx \\ &\times \frac{\sinh(xz)}{\sqrt{x^2 - \mathbf{k}_p^2 - m_{\mathbf{n}_q}^2}} \frac{m \sinh(xz) + x \cosh(xz)}{\frac{x+m}{x-m} e^{2ax} + 1}, \end{aligned} \quad (3.7)$$

where

$$\langle \bar{\psi}\psi \rangle^{(0)} = -\frac{N_D m}{2V_q} \sum_{\mathbf{n}_q \in \mathbf{Z}^q} \int \frac{d\mathbf{k}_{p+1}}{(2\pi)^{p+1}} \frac{1}{\sqrt{\mathbf{k}_{p+1}^2 + m_{\mathbf{n}_q}^2}}, \quad (3.8)$$

is the fermionic condensate in the topology  $R^{p+1} \times (S^1)^q$  when the boundaries are absent. The term

$$\langle \bar{\psi}\psi \rangle^{(1)} = -\frac{N_D}{2\pi V_q} \sum_{\mathbf{n}_q \in \mathbf{Z}^q} \int \frac{d\mathbf{k}_p}{(2\pi)^p} \int_0^\infty dx \frac{x \sin(2xz) - m \cos(2xz)}{\sqrt{x^2 + \mathbf{k}_p^2 + m_{\mathbf{n}_q}^2}}, \quad (3.9)$$

is the part induced by the plate at  $z = 0$  when the second plate is absent. The last term on the right of formula (3.7) comes from the last term in Eq. (3.4) and it is induced by the presence of the second plate. Note that this term vanishes at  $z = 0$ .

For points away from the boundaries, the boundary induced part is finite and the cutoff function in the corresponding expressions can be safely removed. Renormalization is needed for the purely topological part only. The latter has been investigated in Ref. [26] (for the topological fermionic Casimir effect in de Sitter spacetime with toroidally compactified spatial dimensions see Ref. [31]). By making use of the zeta function technique, the corresponding renormalized expression is presented in the form

$$\begin{aligned} \langle \bar{\psi}\psi \rangle^{(0)} &= -\frac{N_D m}{(2\pi)^{(D+1)/2}} \sum'_{\mathbf{n}_q \in \mathbf{Z}^q} \cos(2\pi \mathbf{n}_q \cdot \boldsymbol{\alpha}_q) \\ &\times \frac{f_{(D-1)/2}(m \sqrt{L_{p+2}^2 n_{p+2}^2 + \dots + L_D^2 n_D^2})}{(L_{p+2}^2 n_{p+2}^2 + \dots + L_D^2 n_D^2)^{(D-1)/2}}, \end{aligned} \quad (3.10)$$

with  $\boldsymbol{\alpha}_q = (\alpha_{p+2}, \dots, \alpha_D)$ , and

$$f_\nu(z) = z^\nu K_\nu(z). \quad (3.11)$$

The prime on the summation sign in (3.10) means that the term  $\mathbf{n}_q = 0$  is excluded from the sum. An alternative expression for  $\langle \bar{\psi}\psi \rangle^{(0)}$  is obtained in Ref. [26] using the Abel-Plana summation formula. In the discussion below we will be concentrated on the boundary induced parts.

For further transformation of the single plate part (3.9), we write the function in the integrand as

$$x \sin(2xz) - m \cos(2xz) = -\frac{1}{2} [(m + ix) e^{2ixz} + (m - ix) e^{-2ixz}]. \quad (3.12)$$

In the integral over  $x$  in (3.9) we rotate the integration contour by an angle  $\pi/2$ , for the term with the exponent  $e^{2ixz}$ , and by  $-\pi/2$ , for the term with the exponent  $e^{-2ixz}$ . As a result, we get

$$\langle \bar{\psi}\psi \rangle^{(1)} = \frac{N_D}{2\pi V_q} \sum_{\mathbf{n}_q \in \mathbf{Z}^q} \int \frac{d\mathbf{k}_p}{(2\pi)^p} \int_{\sqrt{\mathbf{k}_p^2 + m_{\mathbf{n}_q}^2}}^\infty dx \frac{(m - x) e^{-2xz}}{\sqrt{x^2 - \mathbf{k}_p^2 - m_{\mathbf{n}_q}^2}}. \quad (3.13)$$

It follows from this expression that  $\langle \bar{\psi}\psi \rangle^{(1)}$  is always negative. By using the relation

$$\int d\mathbf{k}_p \int_{\sqrt{\mathbf{k}_p^2 + m_{\mathbf{n}_q}^2}}^\infty \frac{f(x) dx}{\sqrt{x^2 - \mathbf{k}_p^2 - m_{\mathbf{n}_q}^2}} = \frac{\pi^{(p+1)/2}}{\Gamma((p+1)/2)} \int_{m_{\mathbf{n}_q}}^\infty dx (x^2 - m_{\mathbf{n}_q}^2)^{(p-1)/2} f(x), \quad (3.14)$$

we find

$$\langle \bar{\psi}\psi \rangle^{(1)} = \frac{A_p N_D}{V_q} \sum_{\mathbf{n}_q \in \mathbf{Z}^q} \int_{m_{\mathbf{n}_q}}^\infty dx (x^2 - m_{\mathbf{n}_q}^2)^{(p-1)/2} (m - x) e^{-2xz}, \quad (3.15)$$

with the notation

$$A_p = \frac{(4\pi)^{-(p+1)/2}}{\Gamma((p+1)/2)}. \quad (3.16)$$

The integral in Eq. (3.15) is expressed in terms of the modified Bessel function of the second type, namely

$$\langle \bar{\psi}\psi \rangle^{(1)} = \frac{N_D(2z)^{-p-1}}{(2\pi)^{p/2+1}V_q} \sum_{\mathbf{n}_q \in \mathbf{Z}^q} [2mz f_{p/2}(2m_{\mathbf{n}_q}z) - f_{p/2+1}(2m_{\mathbf{n}_q}z)]. \quad (3.17)$$

In the absence of compact dimensions, from Eq. (3.17) one finds

$$\langle \bar{\psi}\psi \rangle_{R^D}^{(1)} = \frac{N_D(2z)^{-D}}{(2\pi)^{(D+1)/2}} [2mz f_{(D-1)/2}(2mz) - f_{(D+1)/2}(2mz)]. \quad (3.18)$$

Let us consider some limiting cases of the general formula (3.17). In the limit when the length of one of the compactified dimensions, say  $z^j$ ,  $j \geq p+2$ , is large,  $L_j \rightarrow \infty$ , the dominant contribution to the sum over  $n_j$  in Eq. (3.17) comes from large values of  $n_j$  and we can replace the corresponding sum by an integral, with the help of the relation

$$\frac{\pi}{L_j} \sum_{n_j=-\infty}^{+\infty} f(2\pi|n_j + \alpha_j|/L_j) \rightarrow \int_0^\infty dy f(y). \quad (3.19)$$

The integral is evaluated by using the formula

$$\int_0^\infty dy f_\nu(c\sqrt{y^2 + b^2}) = \frac{1}{c} \sqrt{\frac{\pi}{2}} f_{\nu+1/2}(bc),$$

and we can see that, from Eq. (3.17), the corresponding formula is obtained for the topology  $R^{p+2} \times (S^1)^{q-1}$ . At small distances from the boundary,  $z \ll m^{-1}, L_l$ , the main contribution to the series in Eq. (3.17) comes from large values of  $n_l$  and we can replace the summation by the integration and to the leading order we find

$$\langle \bar{\psi}\psi \rangle^{(1)} \approx -\frac{N_D \Gamma((D+1)/2)}{(4\pi)^{(D+1)/2} z^D}. \quad (3.20)$$

This leading behavior does not depend on the lengths of the compact dimensions and, as it is seen from Eq. (3.18), coincides with boundary induced part of the fermionic condensate for a single plate in a space with trivial topology  $R^D$  in the case of a massless field.

Now, let us consider the limit  $L_l \ll z$ . In this case, and for  $\alpha_l = 0$ , the main contribution comes from the zero mode with  $\mathbf{n}_q = 0$  and to the leading order we find

$$\langle \bar{\psi}\psi \rangle^{(1)} \approx \frac{N(2z)^{-p-1}}{(2\pi)^{p/2+1}V_q} [2mz f_{p/2}(2mz) - f_{p/2+1}(2mz)].$$

Comparing with (3.18), we see that the quantity  $V_q \langle \bar{\psi}\psi \rangle_{p,q}^{(1)} / N_D$  coincides with the corresponding result for a plate in topologically trivial  $(p+1)$ -dimensional space,  $R^{p+1}$ . The contribution of the nonzero modes is exponentially suppressed and, for  $\alpha_l \neq 0$ , the zero mode is absent. Assuming that  $mz$  is fixed, to leading order we have

$$\langle \bar{\psi}\psi \rangle^{(1)} = -\frac{N_D m_0^{p+1} e^{-2m_0 z}}{2V_q (4\pi m_0 z)^{(p+1)/2}}, \quad (3.21)$$

where

$$m_0^2 = \sum_{l=p+2}^D (2\pi\alpha_l/L_l)^2. \quad (3.22)$$

In this case, the boundary induced part in the fermionic condensate is exponentially suppressed.

Using (3.14), we can also simplify the expression for the second plate induced part in Eq. (3.7). Combining with Eq. (3.15) we find

$$\begin{aligned} \langle \bar{\psi}\psi \rangle &= \langle \bar{\psi}\psi \rangle^{(0)} - \frac{A_p N_D}{V_q} \sum_{\mathbf{n}_q \in \mathbf{Z}^q} \int_{m_{\mathbf{n}_q}}^{\infty} dx \frac{(x^2 - m_{\mathbf{n}_q}^2)^{(p-1)/2}}{\frac{x+m}{x-m} e^{2ax} + 1} \\ &\times [(m+x)(e^{2xz} + e^{2ax-2xz}) - 2m], \end{aligned} \quad (3.23)$$

where the second term on the rhs is the boundary induced part, which is always negative. For a massless field, by using the expansion  $(e^y + 1)^{-1} = -\sum_{n=1}^{\infty} (-1)^n e^{-ny}$ , from this formula we find

$$\begin{aligned} \langle \bar{\psi}\psi \rangle &= \langle \bar{\psi}\psi \rangle^{(0)} + \frac{2N_D}{(4\pi)^{p/2+1} V_q} \sum_{\mathbf{n}_q \in \mathbf{Z}^q} k_{\mathbf{n}_q}^{p/2+1} \sum_{n=1}^{\infty} (-1)^n \\ &\times \sum_{j=1,2} \frac{K_{p/2+1}(2k_{\mathbf{n}_q}(an - |a_j - z|))}{(an - |a_j - z|)^{p/2}}, \end{aligned} \quad (3.24)$$

where  $a_1 = 0$  and  $a_2 = a$  and where  $k_{\mathbf{n}_q}$  is defined by Eq. (3.6). In the case of trivial topology  $R^D$ , from here we obtain

$$\langle \bar{\psi}\psi \rangle_{R^D} = \frac{N_D \Gamma((D+1)/2)}{(4\pi)^{(D+1)/2} a^D} \sum_{n=1}^{\infty} (-1)^n \left[ \frac{1}{(n - z/a)^D} + \frac{1}{(n - 1 + z/a)^D} \right]. \quad (3.25)$$

The series in these formula are given in terms of the Hurwitz zeta function. The last expression can be further simplified, for odd values of  $D$ , as

$$\langle \bar{\psi}\psi \rangle_{R^D} = -\frac{N_D \Gamma((D+1)/2)}{2^{D+2} \pi^{(D-1)/2} a^D} \frac{d^{D-1}}{dx^{D-1}} \frac{1}{\sin(\pi x)} \Big|_{x=z/a}. \quad (3.26)$$

In the special case  $D = 3$ , from here we obtain the result given in Ref. [23].

Extracting the parts corresponding to the single plates, the fermionic condensate can also be presented in the form

$$\langle \bar{\psi}\psi \rangle = \langle \bar{\psi}\psi \rangle^{(0)} + \sum_{j=1,2} \langle \bar{\psi}\psi \rangle_j^{(1)} + \Delta \langle \bar{\psi}\psi \rangle, \quad (3.27)$$

where  $\langle \bar{\psi}\psi \rangle_j^{(1)}$  is that part in the condensate induced by a single plate located at  $z = a_j$ , with  $a_1 = 0$  and  $a_2 = a$ , and the interference term is given by the expression

$$\begin{aligned} \Delta \langle \bar{\psi}\psi \rangle &= \frac{A_p N_D}{V_q} \sum_{\mathbf{n}_q \in \mathbf{Z}^q} \int_{m_{\mathbf{n}_q}}^{\infty} dx \frac{(x^2 - m_{\mathbf{n}_q}^2)^{(p-1)/2}}{\frac{x+m}{x-m} e^{2ax} + 1} \\ &\times [2m + (x - m)(e^{-2xz} + e^{2xz-2ax})]. \end{aligned} \quad (3.28)$$

As it is seen from this formula, the interference part in the fermionic condensate is always positive. Note that the divergences on the plates are contained in the single plate parts and that

the interference term is finite for all values  $0 \leq z \leq a$ . For a massless field, similar to Eq. (3.24), one finds the expression

$$\Delta\langle\bar{\psi}\psi\rangle = -\frac{2N_D}{(4\pi)^{p/2+1}V_q} \sum_{\mathbf{n}_q \in \mathbf{Z}^q} k_{\mathbf{n}_q}^{p/2+1} \sum_{n=1}^{\infty} (-1)^n \sum_{j=1,2} \frac{K_{p/2+1}(2k_{\mathbf{n}_q}(an + |a_j - z|))}{(an + |a_j - z|)^{p/2}}. \quad (3.29)$$

In the limit  $L_l \ll a$  and for  $\alpha_l = 0$ , the main contribution comes from the zero mode with  $\mathbf{n}_q = 0$  and to leading order we find  $\Delta\langle\bar{\psi}\psi\rangle \approx N_D \Delta\langle\bar{\psi}\psi\rangle_{R^{p+1}} / (N_{p+1} V_q)$ , where

$$\begin{aligned} \Delta\langle\bar{\psi}\psi\rangle_{R^{p+1}} &= A_p N_{p+1} \int_m^\infty dx \frac{(x^2 - m^2)^{(p-1)/2}}{\frac{x+m}{x-m} e^{2ax} + 1} \\ &\times [2m + (x - m)(e^{-2xz} + e^{2xz-2ax})], \end{aligned} \quad (3.30)$$

is the interference part in the fermionic condensate for the geometry of two parallel plates in  $(p + 1)$ -dimensional spacetime with trivial topology  $R^{p+1}$ . When  $\alpha_l \neq 0$ , there is no zero mode and the interference part is exponentially suppressed by the factor  $e^{-2am_0}$ , where  $m_0$  is defined in Eq. (3.22).

In the discussion above we have considered the fermionic condensate in the region between the plates,  $0 < z < a$ . For the regions  $z < 0$  and  $z > a$ , the expression for the fermionic condensate has the form

$$\langle\bar{\psi}\psi\rangle = \langle\bar{\psi}\psi\rangle^{(0)} + \langle\bar{\psi}\psi\rangle^{(1)}, \quad (3.31)$$

where the plate-induced part is given by Eq. (3.17) with the replacement  $z \rightarrow |z|$ , in the region  $z < 0$ , and with the replacement  $z \rightarrow z - a$ , in the region  $z > a$ .

In the presence of a constant gauge field  $A_\mu$ , the corresponding formulas for the fermionic condensate are obtained from those given above by the replacement (2.12). From these formulas it follows that the fermionic condensate is a periodic function of  $A_l L_l$  with the period of the flux quantum  $\Phi_0 = 2\pi/|e|$  ( $\Phi_0 = 2\pi\hbar c/|e|$  in standard units). It is an even function of  $\tilde{\alpha}_l$ .

The formulas corresponding to the special case with a single compact dimension are obtained from those given above by taking  $p = D - 2$ ,  $q = 1$ , and  $k_{\mathbf{n}_q} = 2\pi|n_D + \alpha_D|/L_D$ . In Fig. 1 we plot, for the simplest Kaluza-Klein-type model with spatial topology  $R^3 \times S^1$ , the dependence of the fermionic condensate for a massless fermionic field vs the ratio  $z/a$ , in the region between the plates, for untwisted and twisted fermionic fields, for several values of the ratio  $L/a$ . The dashed lines correspond to the fermionic condensate for the geometry of two plates in a space with topology  $R^4$ , defined by Eq. (3.25). Note that, for a massless field, the pure topological part vanishes. As it is seen from the graphs, for an untwisted (twisted) field the absolute value of the fermionic condensate increases with decreasing (increasing) length of the compact dimension.

## 4 Vacuum expectation value of the energy-momentum tensor

Another important local characteristic of the fermionic vacuum is the VEV of the energy-momentum tensor. In order to find this we use the mode-sum formula

$$\langle T_{\mu\nu} \rangle = \frac{i}{2} \sum_{\beta} [\bar{\psi}_{\beta}^{(-)} \gamma_{(\mu} \partial_{\nu)} \psi_{\beta}^{(-)} - (\partial_{(\mu} \bar{\psi}_{\beta}^{(-)}) \gamma_{\nu)} \psi_{\beta}^{(-)}], \quad (4.1)$$

where the brackets denote the symmetrization over the indices enclosed. By taking into account the expressions for the spinor eigenfunctions, we find the following expressions for the components of the vacuum energy-momentum tensor (no summation over  $\mu$ )

$$\langle T_{\mu}^{\nu} \rangle = -\frac{N_D \delta_{\mu}^{\nu}}{2a V_q} \sum_{\mathbf{n}_q \in \mathbf{Z}^q} \int \frac{d\mathbf{k}_p}{(2\pi)^p} \sum_{n=1}^{\infty} \frac{f^{(\mu)}(\lambda_n)/\omega}{1 - \sin(2\lambda_n)/(2\lambda_n)}, \quad (4.2)$$

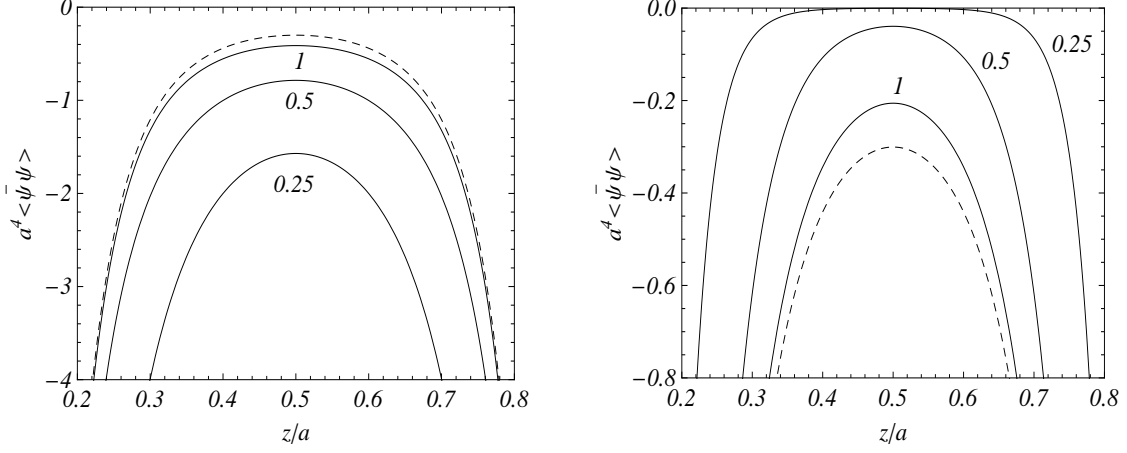


Figure 1: Fermionic condensate between two plates, in the model with spatial topology  $R^3 \times S^1$ , as a function of  $z/a$  for untwisted ( $\alpha_4 = 0$ , left plot) and twisted ( $\alpha_4 = 1/2$ , right plot) fields. The numbers near the curves correspond to the values of the ratio  $L_4/a$ . The dashed lines in both plots correspond to the fermionic condensate for two plates on background of the space with trivial topology  $R^4$  [see Eq. (3.25)].

where  $\omega$  is defined in Eq. (3.3) and

$$\begin{aligned}
f^{(0)}(x) &= \omega^2 [1 - \cos(x) \cos(x(2z^{p+1}/a - 1))], \\
f^{(l)}(x) &= -(k_l^2/\omega^2)f^{(0)}(x), \quad l \neq 0, p+1, \\
f^{(p+1)}(x) &= -k_{p+1}^2.
\end{aligned} \tag{4.3}$$

As in the case of the fermionic condensate, we assume the presence of the cutoff function in (4.2). It can be checked that the VEVs of the separate components obey the trace relation

$$\langle T_\mu^\mu \rangle = m \langle \bar{\psi}\psi \rangle, \tag{4.4}$$

with the fermionic condensate given by Eq. (3.2).

The total vacuum energy (per unit volume along the directions  $z_l$ ,  $l = 1, 2, \dots, p$ ) in the region  $0 < z_{p+1} < a$ ,  $0 \leq z_l \leq L_l$ ,  $l = p+2, \dots, D$ , is obtained integrating  $\langle T_0^0 \rangle$  over this region. By taking into account the expression for the energy density from Eq. (4.2) and Eq. (2.9) for the eigenvalues, we obtain the following expression for the vacuum energy

$$E = -\frac{N_D}{2} \sum_{\mathbf{n}_q \in \mathbf{Z}^q} \int \frac{d\mathbf{k}_p}{(2\pi)^p} \sum_{n=1}^{\infty} \sqrt{\mathbf{k}_p^2 + k_{\mathbf{n}_q}^2 + \lambda_n^2/a^2 + m^2}. \tag{4.5}$$

It coincides with the total energy of the fermionic vacuum in the region under consideration, evaluated as the sum of zero-point energies of elementary oscillators. Hence, we have shown that the vacuum energy obtained by integration of the energy density in the region between the plates does coincide with the energy evaluated as the sum of the zero-point energies of elementary oscillators. This means that the surface energy located on the boundaries is zero for the boundary conditions under consideration. Note that the surface energy vanishes for scalar fields with Dirichlet or Neumann boundary conditions as well, but this is not the case for a scalar field with Robin boundary conditions (see Refs. [29, 32]). The total vacuum energy in

the region between the plates, defined by Eq. (4.5), is investigated in Ref. [16]. Here we will be concerned with the vacuum energy density and stresses.

For the evaluation of the VEVs, given by Eq. (4.2), we apply to the sums over  $n$  the summation formula (3.4). After steps similar to those already described in the case of the fermionic condensate, the VEV of the energy-momentum tensor can be expressed in the decomposed form (no summation over  $\mu$ )

$$\begin{aligned} \langle T_\mu^\nu \rangle &= \langle T_\mu^\nu \rangle^{(0)} + \langle T_\mu^\nu \rangle^{(1)} - \frac{A_p N_D}{V_q} \delta_\mu^\nu \\ &\times \sum_{\mathbf{n}_q \in \mathbf{Z}^q} \int_{m_{\mathbf{n}_q}}^\infty dx \frac{(x^2 - m_{\mathbf{n}_q}^2)^{(p-1)/2}}{\frac{x+m}{x-m} e^{2ax} + 1} F_\mu(x), \end{aligned} \quad (4.6)$$

where  $A_p$  is given by Eq. (3.16) and we have defined the functions

$$\begin{aligned} F_\mu(x) &= \frac{x^2 - m_{\mathbf{n}_q}^2}{p+1} \left( 2 + \frac{m e^{2xz}}{x-m} - \frac{m e^{-2xz}}{x+m} \right), \quad \mu = 0, \dots, p, \\ F_\mu(x) &= k_\mu^2 \left( 2 + \frac{m e^{2xz}}{x-m} - \frac{m e^{-2xz}}{x+m} \right), \quad \mu = p+2, \dots, D, \\ F_\mu(x) &= -2x^2, \quad \mu = p+1. \end{aligned} \quad (4.7)$$

In Eq. (4.6), the term (no summation over  $\mu$ )

$$\langle T_\mu^\nu \rangle^{(0)} = -\frac{N_D \delta_\mu^\nu}{2V_q} \sum_{\mathbf{n}_q \in \mathbf{Z}^q} \int \frac{d\mathbf{k}_{p+1}}{(2\pi)^{p+1}} \frac{f_0^{(\mu)}}{\sqrt{\mathbf{k}_{p+1}^2 + m_{\mathbf{n}_q}^2}}, \quad (4.8)$$

with  $f_0^{(0)} = \mathbf{k}_{p+1}^2 + m_{\mathbf{n}_q}^2$ ,  $f_0^{(l)} = -k_l^2$ ,  $l = 1, \dots, p+1$ , is the VEV of the energy-momentum tensor for the topology  $R^{p+1} \times (S^1)^q$  when the boundaries are absent. This background is homogeneous and the corresponding densities are uniform. The second term on the rhs of Eq. (4.6) is induced by the plate at  $z = 0$  when the second plate is absent (again no summation over  $\mu$ ):

$$\langle T_\mu^\nu \rangle^{(1)} = \frac{N_D m \delta_\mu^\nu}{4\pi V_q} \int \frac{d\mathbf{k}_p}{(2\pi)^p} \sum_{\mathbf{n}_q \in \mathbf{Z}^q} \int_0^\infty dx \frac{f_0^{(\mu)}(x)}{\sqrt{x^2 + \mathbf{k}_p^2 + m_{\mathbf{n}_q}^2}} \left( \frac{e^{-2ixz}}{m+ix} + \frac{e^{2ixz}}{m-ix} \right), \quad (4.9)$$

where

$$\begin{aligned} f_0^{(0)}(x) &= x^2 + \mathbf{k}_p^2 + m_{\mathbf{n}_q}^2, \quad f_0^{(p+1)}(x) = 0, \\ f_0^{(l)}(x) &= -k_l^2, \quad l = 1, \dots, p, p+2, \dots, D. \end{aligned} \quad (4.10)$$

The last term on the rhs of Eq. (4.6) is induced by the presence of the second plate. Note that the vacuum stress along the direction normal to the plates vanishes in the geometry of a single plate and is uniform in the region between the two plates. The renormalized expressions for the purely topological part  $\langle T_\mu^\nu \rangle^{(0)}$  are given in Ref. [26]. In particular, for the corresponding energy density one has

$$\begin{aligned} \langle T_0^0 \rangle^{(0)} &= \frac{N_D}{(2\pi)^{(D+1)/2}} \sum'_{\mathbf{n}_q \in \mathbf{Z}^q} \cos(2\pi \mathbf{n}_q \cdot \tilde{\boldsymbol{\alpha}}_q) \\ &\times \frac{f_{(D+1)/2}(m \sqrt{L_{p+2}^2 n_{p+2}^2 + \dots + L_D^2 n_D^2})}{(L_{p+2}^2 n_{p+2}^2 + \dots + L_D^2 n_D^2)^{(D+1)/2}}. \end{aligned} \quad (4.11)$$

where, as before, the prime means that the term  $\mathbf{n}_q = 0$  is excluded from the sum. Note that (no summation over  $\mu$ )  $\langle T_\mu^\mu \rangle^{(0)} = \langle T_0^0 \rangle^{(0)}$  for  $\mu = 1, \dots, p+1$ . In the discussion below we will be concerned with the boundary induced parts.

The single plate part, Eq. (4.9), can be further simplified. With this aim, in the term with the exponent  $e^{2ixz}$  ( $e^{-2ixz}$ ), we rotate the integration contour in the complex plane  $x$  by the angle  $\pi/2$  ( $-\pi/2$ ). By using the integration formula (3.14), we find the following result (no summation over  $\mu$ )

$$\langle T_\mu^\mu \rangle^{(1)} = -m \frac{A_p N_D}{V_q} \sum_{\mathbf{n}_q \in \mathbf{Z}^q} \int_{m_{\mathbf{n}_q}}^{\infty} dx \frac{(x^2 - m_{\mathbf{n}_q}^2)^{(p-1)/2}}{(x+m)e^{2xz}} F_0^{(\mu)}(x), \quad (4.12)$$

with the notations

$$\begin{aligned} F_0^{(\mu)}(x) &= \frac{x^2 - m_{\mathbf{n}_q}^2}{p+1}, \quad \mu = 0, 1, \dots, p, \\ F_0^{(\mu)}(x) &= k_\mu^2, \quad \mu = p+2, \dots, D, \end{aligned} \quad (4.13)$$

and  $F_0^{(p+1)}(x) = 0$ . Note that the boundary induced parts in the vacuum stresses along the uncompactified directions parallel to the plates are equal to the boundary induced part in the energy density. This result is a consequence of the Lorentz invariance of the problem along these directions. The energy density is negative everywhere. In the absence of compact dimensions, from Eq. (4.12) one finds (no summation over  $\mu$ )

$$\langle T_\mu^\mu \rangle^{(1)} = m \langle \bar{\psi} \psi \rangle^{(1)} / D, \quad (4.14)$$

for  $\mu = 0, \dots, D-1$ , and  $\langle T_D^D \rangle^{(1)} = 0$ . In Eq. (4.14)  $\langle \bar{\psi} \psi \rangle^{(1)}$  is given by Eq. (3.18). Of course, Eq. (4.14) is a direct consequence of the trace relation (4.4).

When the length of the  $j$ -th compact dimension is large, we replace the summation over  $n_j$  in Eq. (4.12) by an integral, with the help of Eq. (3.19). As next step, we introduce a new integration variable  $v = \sqrt{x^2 - m_{\mathbf{n}_q}^2}$ . After changing to polar coordinates in the  $(y, v)$ -plane, the angular part of the integral is evaluated explicitly and, as it can be seen from Eq. (4.12), to leading order the result is obtained for the topology  $R^{p+2} \times (S^1)^{q-1}$ .

For points near the plate,  $z \ll L_l$ , the dominant contribution to the series in Eq. (4.12) comes from large values of  $n_l$ . Replacing the corresponding summations by integrations, we see that, to leading order, the behavior of the VEV coincides with the one for topologically trivial space. If, in addition,  $z \ll m^{-1}$ , combining Eq. (4.14) with Eq. (3.20), one finds (no summation over  $\mu$ )

$$\langle T_\mu^\mu \rangle^{(1)} \approx -\frac{m N_D \Gamma((D+1)/2)}{(4\pi)^{(D+1)/2} D z^D}, \quad (4.15)$$

for  $\mu = 0, \dots, D-1$ . For  $L_l \ll z$  the behavior of the VEVs is essentially different, depending on the phases  $\alpha_l$  in the periodicity conditions. When  $\alpha_l = 0$ ,  $l = 0, \dots, D$ , the contribution of the nonzero modes is exponentially suppressed and the dominant contribution comes from the zero mode  $\mathbf{n}_q = 0$ . For the components along the uncompactified dimensions, to leading order we have (no summation over  $\mu$ )  $\langle T_\mu^\mu \rangle^{(1)} \approx N_D \langle T_\mu^\mu \rangle_{R^{p+1}}^{(1)} / (V_q N_{p+1})$ ,  $\mu = 0, \dots, p+1$ , where  $\langle T_\mu^\nu \rangle_{R^{p+1}}^{(1)}$  is the corresponding VEV for two parallel plates in the space  $R^{p+1}$  located at  $z = 0$  and  $z = a$ . For the stress along the  $l$ -th compact dimension the contribution of the zero mode vanishes and, in the case under consideration ( $\alpha_l = 0$ ), the dominant contribution comes from the modes with  $n_l = \pm 1$ ,  $n_j = 0$ ,  $j \neq l$ , and the stress is exponentially suppressed (no summation over  $l$ ):

$\langle T_l^l \rangle^{(1)} \propto e^{-2z/L_l}$ . We have also assumed that  $L_l \ll m^{-1}$ . For  $\alpha_l \neq 0$  the VEVs are exponentially suppressed and to leading order we have (no summation over  $\mu$ )

$$\langle T_\mu^\mu \rangle^{(1)} \approx -\frac{(4\pi)^{-(p+1)/2} N_D m m_0^{p+1}}{4V_q (m_0 z)^{(p+3)/2} e^{2m_0 z}}, \quad (4.16)$$

for  $\mu = 0, \dots, p$  and  $m_0$  one recovers Eq. (3.22). We have a similar exponential suppression for the stresses along the compact dimensions.

Now we return to the two plate geometry. Combining Eq. (4.12) with Eq. (4.6), for the VEV of the energy-momentum tensor in the region between the plates, we find (no summation over  $\mu$ )

$$\langle T_\mu^\nu \rangle = \langle T_\mu^\nu \rangle^{(0)} - \delta_\mu^\nu \frac{A_p N_D}{V_q} \sum_{\mathbf{n}_q \in \mathbf{Z}^q} \int_{m_{\mathbf{n}_q}}^\infty dx \frac{(x^2 - m_{\mathbf{n}_q}^2)^{(p-1)/2}}{\frac{x+m}{x-m} e^{2ax} + 1} G_\mu(x), \quad (4.17)$$

where

$$G_\mu(x) = \frac{x^2 - m_{\mathbf{n}_q}^2}{p+1} \left[ 2 + \frac{m}{x-m} (e^{2xz} + e^{2ax-2xz}) \right], \quad \mu = 0, 1, \dots, p, \quad (4.18)$$

$$G_\mu(x) = k_\mu^2 \left[ 2 + \frac{m}{x-m} (e^{2xz} + e^{2ax-2xz}) \right], \quad \mu = p+2, \dots, D, \quad (4.19)$$

and  $G_{p+1}(x) = F_{p+1}(x)$ . From here, it follows that the boundary induced part in the vacuum energy density is always negative. It can be easily checked that the boundary induced parts obey the trace relation (4.4). For the VEV in the geometry of two parallel plates located at  $z = 0$  and  $z = a$  in a  $D$ -dimensional space with topology  $R^D$ , one has (no summation over  $\mu$ )

$$\langle T_\mu^\nu \rangle_{R^D} = -\frac{N_D \delta_\mu^\nu}{(4\pi)^{D/2} \Gamma(D/2)} \int_m^\infty dx \frac{(x^2 - m^2)^{(p-1)/2}}{\frac{x+m}{x-m} e^{2ax} + 1} G_{0\mu}(x), \quad (4.20)$$

where the expression for  $G_{0\mu}(x)$ , with  $\mu = 0, 1, \dots, D-1$ , is obtained from Eq. (4.18) by the replacement  $m_{\mathbf{n}_q} \rightarrow m$  and  $G_{0D}(x) = -2x^2$ . For a massless field this result reduces to

$$\langle T_\mu^\nu \rangle_{R^D} = -\frac{(1 - 2^{-D}) N_D}{(4\pi)^{(D+1)/2} a^{D+1}} \zeta(D+1) \Gamma((D+1)/2) \text{diag}(1, \dots, 1, -D). \quad (4.21)$$

Note that  $\langle T_\mu^\nu \rangle_{R^D} = (1 - 2^{-D}) N_D \langle T_\mu^\nu \rangle_{R^D}^{(\text{sc})}$ , where  $\langle T_\mu^\nu \rangle_{R^D}^{(\text{sc})}$  is the corresponding VEV for a scalar field with Dirichlet or Neumann boundary conditions on the plates.

For a massless field and in the presence of compact dimensions, the expressions for the VEV of the energy-momentum tensor are obtained from general formulas (4.17) by putting  $m = 0$ . Alternative expressions are derived using the expansion  $(e^y + 1)^{-1} = -\sum_{n=1}^\infty (-1)^n e^{-ny}$ . After integration one finds (no summation over  $\mu$ )

$$\langle T_\mu^\mu \rangle = \langle T_\mu^\mu \rangle^{(0)} + \frac{2N_D}{(2\pi)^{p/2+1} V_q} \sum_{n=1}^\infty \frac{(-1)^n}{(2an)^{p+2}} \sum_{\mathbf{n}_q \in \mathbf{Z}^q} G_\mu^{(0)}(2ank_{\mathbf{n}_q}), \quad (4.22)$$

with the notations

$$\begin{aligned} G_\mu^{(0)}(x) &= f_{p/2+1}(x), \quad \mu = 0, \dots, p, \\ G_\mu^{(0)}(x) &= (2ank_\mu)^2 f_{p/2}(x), \quad \mu = p+2, \dots, D, \\ G_{p+1}^{(0)}(x) &= -(p+1) f_{p/2+1}(x) - x^2 f_{p/2}(x). \end{aligned} \quad (4.23)$$

The corresponding vacuum densities are uniform. In this case the boundary induced part in the total energy (per unit volume along uncompactified dimensions) of the vacuum is  $aV_q\Delta\langle T_0^0\rangle$  and the corresponding result obtained from Eq. (4.22) coincides with the result derived in Ref. [16] by using zeta function techniques.

Similar to Eq. (3.27), the VEV of the energy-momentum tensor may be presented in the decomposed form

$$\langle T_\mu^\nu\rangle = \langle T_\mu^\nu\rangle^{(0)} + \sum_{j=1,2} \langle T_\mu^\nu\rangle_j^{(1)} + \Delta\langle T_\mu^\nu\rangle, \quad (4.24)$$

where  $\langle T_\mu^\nu\rangle_j^{(1)}$  is the part in the VEV induced by a single plate at  $z = a_j$ , with  $a_1 = 0$ ,  $a_2 = a$ . The interference part in Eq. (4.6) is given by the expression (no summation over  $\mu$ )

$$\Delta\langle T_\mu^\nu\rangle = -\delta_\mu^\nu \frac{A_p N_D}{V_q} \sum_{\mathbf{n}_q \in \mathbf{Z}^q} \int_{m_{\mathbf{n}_q}}^\infty dx \frac{(x^2 - m_{\mathbf{n}_q}^2)^{(p-1)/2}}{\frac{x+m}{x-m} e^{2ax} + 1} H_\mu(x), \quad (4.25)$$

with the notation

$$\begin{aligned} H_\mu(x) &= \frac{x^2 - m_{\mathbf{n}_q}^2}{p+1} \left[ 2 - \frac{m}{x+m} \left( e^{-2xz} + e^{-2x(a-z)} \right) \right], \quad \mu = 0, 1, \dots, p, \\ H_\mu(x) &= k_\mu^2 \left[ 2 - \frac{m}{x+m} \left( e^{-2xz} + e^{-2x(a-z)} \right) \right], \quad \mu = p+2, \dots, D, \end{aligned} \quad (4.26)$$

and  $H_{p+1}(x) = F_{p+1}(x)$ . The surface divergences in the VEV of the energy-momentum tensor are contained in the single plate parts only and the interference part is everywhere finite. For a massless field, the single plate parts in the VEV of the energy-momentum tensor vanish and the interference part coincides with the second term on the rhs of Eq. (4.22). In the limit  $L_l \ll a$  and for  $\alpha_l = 0$  the dominant contribution to the interference part comes from the zero mode  $\mathbf{n}_q$ . To leading order, we find (no summation over  $\mu$ )  $\Delta\langle T_\mu^\mu\rangle = N_D \Delta\langle T_\mu^\mu\rangle_{R^{p+1}} / (V_q N_{p+1})$ ,  $\mu = 0, 1, \dots, p+1$ , where  $\Delta\langle T_\mu^\mu\rangle_{R^{p+1}}$  is the VEV for two plates in a  $(p+1)$ -dimensional spacetime with topology  $R^{p+1}$ . For the stress along the  $l$ -th compact dimension, the contribution of the zero mode vanishes. The dominant contribution comes from the modes with  $n_l = \pm 1$ ,  $n_j = 0$ ,  $j \neq l$ , and the stress is exponentially suppressed:  $\Delta\langle T_l^l\rangle \propto e^{-2a/L_l}$ , where we have additionally assumed that  $L_l \ll m^{-1}$ . For  $\alpha_l \neq 0$  and  $L_l \ll a$  the interference part in the VEV of the energy-momentum tensor is suppressed by the factor  $e^{-2am_0}$ , with  $m_0$  defined in Eq. (3.22).

In the regions  $z^{p+1} < 0$  and  $z^{p+1} > a$  the expression for the VEV of the energy-momentum tensor has the form

$$\langle T_\mu^\nu\rangle = \langle T_\mu^\nu\rangle^{(0)} + \langle T_\mu^\nu\rangle^{(1)}, \quad (4.27)$$

where the boundary induced part is given by Eq. (4.12), with the replacements  $z \rightarrow |z|$  and  $z \rightarrow z - a$  for the regions  $z < 0$  and  $z > a$ , respectively. In the presence of a constant gauge field  $A_\mu$ , the formulas for the VEV of the energy-momentum tensor are obtained by the replacement (2.12). As in the case of the fermionic condensate, the vacuum energy-momentum tensor is a periodic function of  $A_l L_l$  with the period of the flux quantum.

The vacuum forces per unit surface of the plates are equal to the normal stress evaluated at  $z = 0$  and  $z = a$ . By taking into account that  $\langle T_{p+1}^{p+1}\rangle^{(1)} = 0$  one finds, in the region between the plates,

$$\begin{aligned} P(0+) &= P(a-) = -\langle T_{p+1}^{p+1}\rangle^{(0)} - \Delta\langle T_{p+1}^{p+1}\rangle \\ &= -\langle T_{p+1}^{p+1}\rangle^{(0)} - \frac{2A_p N_D}{V_q} \sum_{\mathbf{n}_q \in \mathbf{Z}^q} \int_{\tilde{m}_{\mathbf{n}_q}}^\infty dx \frac{x^2 (x^2 - \tilde{m}_{\mathbf{n}_q}^2)^{(p-1)/2}}{\frac{x+m}{x-m} e^{2ax} + 1}, \end{aligned} \quad (4.28)$$

where  $\tilde{m}_{\mathbf{n}_q}^2 = \sum_{l=p+2}^D [2\pi(n_l + \tilde{\alpha}_l)/L_l]^2 + m^2$ . The term  $-\langle T_{p+1}^{p+1} \rangle^{(0)}$  does not depend on the plate separation, it is a purely topological part in the vacuum forces. For this term, one has  $\langle T_{p+1}^{p+1} \rangle^{(0)} = \langle T_0^0 \rangle^{(0)}$ , with  $\langle T_0^0 \rangle^{(0)}$  given by Eq. (4.11). The last term on the rhs of Eq. (4.28) is induced by the presence of the second plate and determines the interaction forces between the plates. This term is negative and the interaction forces between the plates are always attractive, with independence of the periodicity conditions along compact dimensions and of the value of the gauge potential. In absence of the gauge field, Eq. (4.28) coincides with the result obtained in Ref. [16], by differentiation of the total Casimir energy. For the vacuum forces in the regions  $z < 0$  and  $z > a$ , only the pure topological part contributes, and one has

$$P(0-) = P(a+) = -\langle T_{p+1}^{p+1} \rangle^{(0)}. \quad (4.29)$$

When the quantum field lives in all regions, the pure topological parts of the force acting from the left and from the right-hand sides of the plate compensate and the resulting force is determined by the last term on the rhs of Eq. (4.28). In some important physical situations (bag model in QCD, finite-length carbon nanotubes, higher-dimensional models with orbifolded extra dimensions) the quantum field is confined to the interior of some region and there is no field outside. For the problem under consideration, if the quantum field is confined in the region between the plates, the total Casimir force, acting per unit surface of the plate, is determined by Eq. (4.28) and the pure topological part contributes as well. The resulting force can be either attractive or repulsive, depending on the phases in the periodicity conditions along the compact dimensions, and also on the gauge potential. In this case, the Casimir effect could be used as a stabilization mechanism for both the interplate distance and the size of the compact subspace in Kaluza-Klein-type models and in braneworlds. This is a quite remarkable and very useful result, because this force could be, in principle, easily controlled.

In Fig. 2, we have plotted the ratio of the boundary induced part in the Casimir energy (per unit surface along uncompactified dimensions) for two parallel plates in the spacetime with topology  $R^3 \times S^1$  by the Casimir energy in  $R^3$ ,  $E_{R^3 \times S^1}^{(b)}/E_{R^3} = L\langle T_0^0 \rangle^{(b)}/\langle T_0^0 \rangle_{R^3}$  ( $L$  being the length of the compact dimension), with  $\langle T_0^0 \rangle^{(b)} = \langle T_0^0 \rangle - \langle T_0^0 \rangle^{(0)}$ , for a massless fermionic field, as a function of  $a/L$ . The values on each of the curves correspond to those of the parameter  $\alpha_4$ . Note that from Eq. (4.21) one has  $\langle T_0^0 \rangle_{R^3} = -7\pi^2/(2880a^4)$ . The feature described before is apparent: for large values of  $a/L$  the Casimir energy is suppressed for  $\alpha_4 \neq 0$ .

For a massless case the fermionic field is conformally invariant. We can generate the corresponding VEVs in conformally flat spacetimes by using standard conformal transformation techniques (see, for instance, [28]) and the formulas given above. Consider a conformally-flat spacetime with the line-element

$$ds^2 = \Omega^2(z_l)(dt^2 - \sum_{i=1}^D (dz_i)^2), \quad (4.30)$$

and spatial topology  $R^{p+1} \times (S^1)^q$ , with  $0 \leq z_l \leq L_l$ ,  $l = p+2, \dots, D$ . As before, we assume the presence of two boundaries located at  $z = 0$  and  $z = a$  ( $z_{p+1} \equiv z$ ), with the boundary conditions  $[1 + i\gamma_{(\Omega)}^\mu n_{(\Omega)\mu}] \psi_{(\Omega)} = 0$ , where the subscript  $\Omega$  specifies the quantities on the background described by Eq. (4.30). For curved space gamma matrices we have  $\gamma_{(\Omega)}^\mu = e_l^\mu \gamma^l$ , with the tetrad field  $e_l^\mu = \Omega^{-1} \delta_l^\mu$ . By taking into account that, under the conformal transformation for a massless field, one has  $\psi_{(\Omega)} = \Omega^{-D} \psi$  and  $n_{(\Omega)\mu} = \Omega n_\mu$ , we see that the MIT bag boundary condition is conformally invariant. For the fermionic condensate and the VEV of the energy-momentum

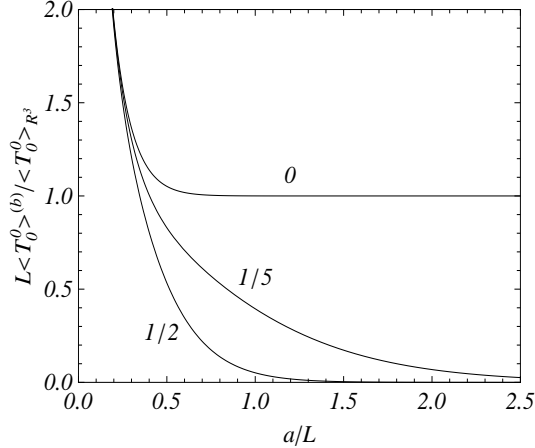


Figure 2: Ratio of the boundary induced part in the Casimir energy for two parallel plates in the spacetime with spatial topology  $R^3 \times S^1$  by the standard Casimir energy in  $R^3$ , for a massless fermionic field, as a function of  $a/L$ . The values on each of the curves correspond to those of the parameter  $\alpha_4$ .

tensor on the spacetime (4.30), one finds

$$\begin{aligned} \langle \bar{\psi}\psi \rangle_{(\Omega)} &= \langle \bar{\psi}\psi \rangle_{(\Omega),R^D} + \Omega^{-D} \langle \bar{\psi}\psi \rangle, \\ \langle T_\mu^\nu \rangle_{(\Omega)} &= \langle T_\mu^\nu \rangle_{(\Omega),R^D} + \Omega^{-D-1} \langle T_\mu^\nu \rangle, \end{aligned} \quad (4.31)$$

where  $\langle \bar{\psi}\psi \rangle_{(\Omega),R^D}$  and  $\langle T_\mu^\nu \rangle_{(\Omega),R^D}$  are the corresponding VEVs for spacetime (4.30) with trivial spatial topology  $R^D$ . Note that for points away from the boundaries, all divergences are contained in these terms and the renormalization procedure is needed for them only. The second terms on the rhs of Eq. (4.31) are induced by the non-trivial topology and by the boundaries. Most important special cases of Eq. (4.30) are the de Sitter (dS) and the anti-de Sitter (AdS) spacetimes, with  $\Omega_{\text{dS}}^2 = 1/(Ht)^2$  and  $\Omega_{\text{AdS}}^2 = 1/(kz)^2$ , described in the inflationary and Poincare coordinates, respectively. In particular, the results for AdS bulk can be applied to massless Dirac fields in higher-dimensional Randall-Sundrum-type braneworld models with two branes and with compact internal spaces.

## 5 Casimir densities in carbon nanotubes

In a significant variety of planar condensed matter systems, the low-energy sector is very well described by the Dirac-like model. A well-known example is the important case of graphene. In this section we apply general results obtained above for electrons in cylindrical nanotubes of finite length. Recently, carbon nanotubes have attracted a lot of attention due to the experimental observation in them of a number of novel electronic properties, what renders them very important for technological purposes. A single-wall cylindrical nanotube is a graphene sheet rolled into a cylindrical shape. The low-energy excitations of the electronic subsystem in a graphene sheet can be described by a pair of two-component spinors,  $\psi_A$  and  $\psi_B$ , corresponding to the two different triangular sublattices of the honeycomb lattice of graphene (see, for instance, [2, 3]). The Dirac equation for these spinors has the form

$$(iv_F^{-1}\gamma^0 D_0 + i\gamma^l D_l - m)\psi_J = 0, \quad (5.1)$$

where  $J = A, B$ ,  $l = 1, 2$ , and  $D_\mu = \partial_\mu + ieA_\mu$  with  $e = -|e|$  for electrons. In Eq. (5.1),  $v_F \approx 10^8$  cm/s represents the Fermi velocity which plays the role of the speed of light. To make the treatment more general, we have included in Eq. (5.1) the mass (gap) term. The gap in the energy spectrum is essential for many physical applications. It can be generated by a number of mechanisms (see, for example, [3, 33, 34, 35, 36]). In particular, they include the breaking of symmetry between two sublattices by introducing a staggered onsite energy [3], the phenomenon of magnetic catalysis [33], and the deformations of bonds in the graphene lattice [34]. Another approach is to attach a graphene monolayer to a substrate, the interaction with which breaks the sublattice symmetry [35]. Note that the Casimir interaction between graphene sheets, resulting from the quantum fluctuations of the bulk electromagnetic field, has been recently investigated in Ref. [37] (for the comparison of the results based on the hydrodynamic and Dirac models of dispersion for graphene, see Ref. [38]).

For the geometry of a carbon nanotube the spatial topology is  $R^1 \times S^1$ . The nanotube is characterized by its chiral vector  $\mathbf{C}_h = n_w \mathbf{a}_1 + m_w \mathbf{a}_2$ , where  $n_w, m_w$  are integers,  $\mathbf{a}_1$  and  $\mathbf{a}_2$  are the basis vectors of the hexagonal lattice of graphene and  $a = |\mathbf{a}_1| = |\mathbf{a}_2| = 2.46 \text{ \AA}$  is the lattice constant. For the length of the compact dimension, one has  $L = |\mathbf{C}_h| = a\sqrt{n_w^2 + m_w^2 + n_w m_w}$ , where for zigzag and armchair nanotubes,  $\mathbf{C}_h = (n_w, 0)$  and  $\mathbf{C}_h = (n_w, n_w)$ , respectively. All other cases correspond to chiral nanotubes. In the case  $n_w - m_w = 3q_w$ ,  $q_w \in Z$ , the nanotube will be metallic and in the case  $n_w - m_w \neq 3q_w$  the nanotube will be a semiconductor with an energy gap inversely proportional to its diameter. We will assume that the nanotube has finite length,  $a$ . As the Dirac field lives on the cylinder surface, it is natural to impose bag boundary conditions (2.2) on the cylinder edges which insure a zero fermion flux through these edges. The additional confinement of the fermionic field along the tube axis leads to the change of the VEVs. The corresponding expressions for the fermionic condensate and the energy-momentum tensor are obtained from the formulas of the previous sections, taking  $D = 2$ ,  $p = 0$ ,  $q = 1$ . The periodicity condition along the compact dimension for the fields  $\psi_J$  depends on the chirality of the nanotube. For metallic nanotubes, we have periodic boundary condition ( $\alpha_l = 0$ ) and for semiconductor nanotubes, depending on the chiral vector, there are two classes of inequivalent boundary conditions, corresponding to  $\alpha_l = \pm 1/3$ . These phases have opposite signs for the sublattices  $A$  and  $B$ . The presence of the gauge field in Eq. (5.1) leads to an Aharonov-Bohm effect in carbon nanotubes [39]. This effect manifests itself in a periodic energy gap modulation and conductance oscillations, as a function of the enclosed magnetic flux, with a period of the order of the flux quantum. As we will see below, similar oscillations arise for the fermionic condensate and Casimir densities.

First, we consider the fermionic condensate (see Ref. [40] for the fermionic condensate and VEV of the fermionic current in a  $(2 + 1)$ -dimensional conical spacetime, in the presence of a circular boundary). The corresponding expression is obtained from the formulas in Sect. 3 taking  $p = 0$ ,  $D = 2$  and summing the contributions coming from the two sublattices with opposite signs of  $\alpha_2 \equiv \alpha$ . For an infinite carbon nanotube, from Eq. (3.10) one has, for the pure topological part,

$$\langle \bar{\psi}\psi \rangle_{\text{cn}}^{(0)} = -\frac{2mv_F}{\pi L} \sum_{n=1}^{\infty} \frac{e^{-nmL}}{n} \cos(2\pi n\alpha) \cos(2\pi n\Phi/\Phi_0), \quad (5.2)$$

where  $\Phi = A_2 L$  is the magnetic flux across the nanotube and  $\alpha = 0, 1/3$  for a metallic and for a semiconducting nanotube, respectively. In the case of a nanotube of finite length,  $a$ , the general expression (3.23) takes the form

$$\langle \bar{\psi}\psi \rangle_{\text{cn}} = \langle \bar{\psi}\psi \rangle_{\text{cn}}^{(0)} - \frac{v_F}{\pi L} \sum_{n=-\infty}^{+\infty} \sum_{j=+,-} \int_{m_n^{(j)}}^{\infty} dx \frac{(m+x)(e^{2xz} + e^{2ax-2xz}) - 2m}{\sqrt{x^2 - m_n^{(j)2}} \left( \frac{x+m}{x-m} e^{2ax} + 1 \right)}, \quad (5.3)$$

with the notation

$$m_n^{(\pm)} = \sqrt{k_n^{(\pm)2} + m^2}, \quad k_n^{(\pm)} = 2\pi|n + \alpha \pm \Phi/\Phi_0|/L. \quad (5.4)$$

Note that for metallic nanotubes the contribution of the terms with  $j = +$  and  $j = -$  coincide. In the absence of the magnetic flux, the sublattices give the same contribution to the condensate. For a massless field the purely topological part vanishes and the boundary induced part reduces to

$$\langle \bar{\psi}\psi \rangle_{\text{cn}} = \frac{1}{\pi L} \sum_{n=-\infty}^{+\infty} \sum_{j=+,-} k_n^{(j)} \sum_{l=1}^{\infty} (-1)^l [K_1(2k_n^{(j)}(al - z)) + K_1(2k_n^{(j)}(al - a + z))]. \quad (5.5)$$

As already mentioned, the condensate is a periodic function of the magnetic flux, with period equal to the flux quantum  $\Phi_0$ . Various important limiting cases directly follow from the analysis given above.

Now we turn to the VEV of the energy-momentum tensor. For the pure topological part, we have the expression (no summation over  $\mu$ )

$$\langle T_\mu^\nu \rangle_{\text{cn}}^{(0)} = \frac{2v_F \delta_\mu^\nu}{\pi L^3} \sum_{n=1}^{\infty} \cos(2\pi n \alpha) \cos(2\pi n \Phi/\Phi_0) C_\mu(nmL) \frac{e^{-nmL}}{n^3}, \quad (5.6)$$

with the notations

$$C_0(x) = C_1(x) = 1 + x, \quad C_2(x) = -2 - 2x - x^2. \quad (5.7)$$

In particular, in absence of magnetic flux, the corresponding energy density is positive for metallic nanotubes and negative for semiconducting ones. This means that, from the topological viewpoint, semiconducting nanotubes are more stable. For a finite length nanotube, from Eq. (4.17) we find the following expression (no summation over  $\mu$ )

$$\langle T_\mu^\nu \rangle_{\text{cn}} = \langle T_\mu^\nu \rangle_{\text{cn}}^{(0)} - \frac{v_F \delta_\mu^\nu}{\pi L} \sum_{n=-\infty}^{+\infty} \sum_{j=+,-} \int_{m_n^{(j)}}^{\infty} dx \frac{(x^2 - m_n^{(j)2})^{-1/2}}{\frac{x+m}{x-m} e^{2ax} + 1} G_\mu^{(j)}(x), \quad (5.8)$$

where

$$\begin{aligned} G_0^{(j)}(x) &= (x^2 - m_n^{(j)2}) \left[ 2 + \frac{m}{x-m} (e^{2xz} + e^{2ax-2xz}) \right], \\ G_1^{(j)}(x) &= -2x^2, \\ G_2^{(j)}(x) &= k_n^{(j)2} \left[ 2 + \frac{m}{x-m} (e^{2xz} + e^{2ax-2xz}) \right]. \end{aligned} \quad (5.9)$$

In absence of magnetic flux, the energy density corresponding to Eq. (5.8) is always negative for semiconducting nanotubes. For metallic nanotubes the energy density is positive for long tubes and negative for short ones. The forces acting on the tube edges are determined by the component  $\langle T_1^1 \rangle_{\text{cn}}$ . As already explained before, the force corresponding to the second term on the rhs of Eq. (5.8) is attractive, with independence of the nanotube chirality and of the magnetic flux. This term dominates for short nanotubes. As regards the first term, it dominates for long tubes and, in the absence of magnetic flux, it corresponds to the attractive force for metallic nanotubes and to the repulsive force for semiconducting ones. Hence, in absence of a magnetic flux, the resulting force is always attractive for metallic nanotubes, whereas for semiconducting ones the force is attractive for short tubes and repulsive for long ones. The sign of the force for long nanotubes can be simply controlled by tuning up the magnetic flux. This result is again of high technological importance.

In the massless case, the above formulas take the form (no summation over  $\mu$ )

$$\langle T_\mu^\nu \rangle_{\text{cn}} = \langle T_\mu^\nu \rangle_{\text{cn}}^{(0)} + \frac{2v_F \delta_\mu^\nu}{\pi L} \sum_{s=1}^{\infty} \frac{(-1)^s}{(2as)^2} \sum_{j=+,-} \sum_{n=-\infty}^{+\infty} G_\mu^{(0)}(2sak_n^{(j)}), \quad (5.10)$$

with the notations

$$\begin{aligned} G_0^{(0)}(x) &= xK_1(x), \quad G_2^{(0)}(x) = x^2K_0(x), \\ G_1^{(0)}(x) &= -xK_1(x) - x^2K_0(x). \end{aligned} \quad (5.11)$$

In Fig. 3 we have plotted the vacuum energy density and vacuum stresses for a massless fermionic field in metallic nanotubes as functions of the tube length in absence of magnetic flux,  $a_0$  being an arbitrary length scale.

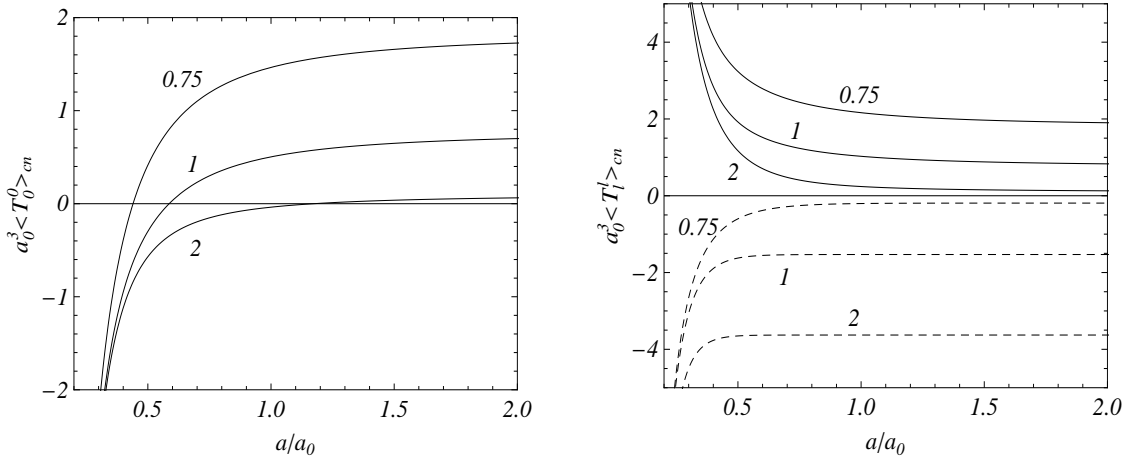


Figure 3: VEV of the energy density (left plot) and vacuum stresses (right plot) for a metallic nanotube, as functions of the tube length, for several values of its circumference,  $L/a_0$  (numbers near the curves). On the left plot full/dashed curves correspond to  $l = 1/l = 2$ , respectively.

For long tubes the pure topological part dominates in the VEV of the energy density and in the case of the values for parameters corresponding to Fig. 3 one has:

$$\langle T_l^l \rangle_{\text{cn}} \approx \langle T_l^l \rangle_{\text{cn}}^{(0)} = \frac{2v_F \zeta(3)}{\pi L^3} \text{diag}(1, 1, -2), \quad (5.12)$$

with  $\zeta(3) \approx 1.202$ . The effective pressure on the tube edges is defined by  $-\langle T_1^1 \rangle_{\text{cn}}$  and, as seen from the right plot, it is always negative, corresponding to attractive forces between the edges for metallic nanotubes.

Fig. 4 is a corresponding plot of the VEVs of the energy density and stresses for semiconducting nanotubes ( $\alpha = 1/3$ ), for a massless field in the absence of magnetic flux. Now, for long tubes we have the limiting value

$$\langle T_l^l \rangle_{\text{cn}} \approx \langle T_l^l \rangle_{\text{cn}}^{(0)} = -\frac{0.340v_F}{L^3} \text{diag}(1, 1, -2). \quad (5.13)$$

The forces acting on the tube edges are attractive at small distances and repulsive at large distances.

In Fig. 5 we have plotted the vacuum energy density as a function of the magnetic flux for metallic (left plot) and semiconducting (right plot) nanotubes, respectively. Recall that the vacuum densities are periodic functions of the magnetic flux, with period equal to the flux quantum. The numbers labelling the curves correspond to the values of the ratio  $L/a$ .

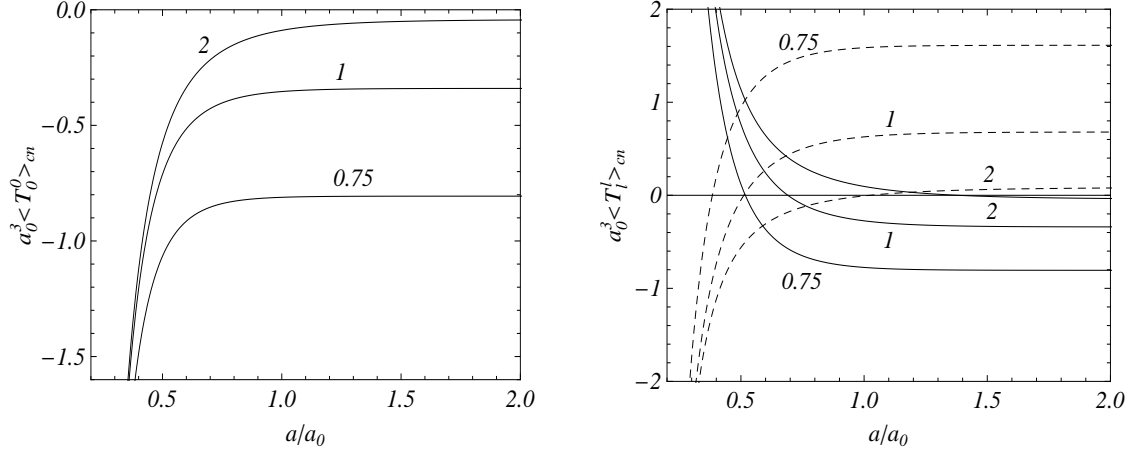


Figure 4: The same as in figure 3 for semiconducting nanotube ( $\alpha = 1/3$ ).

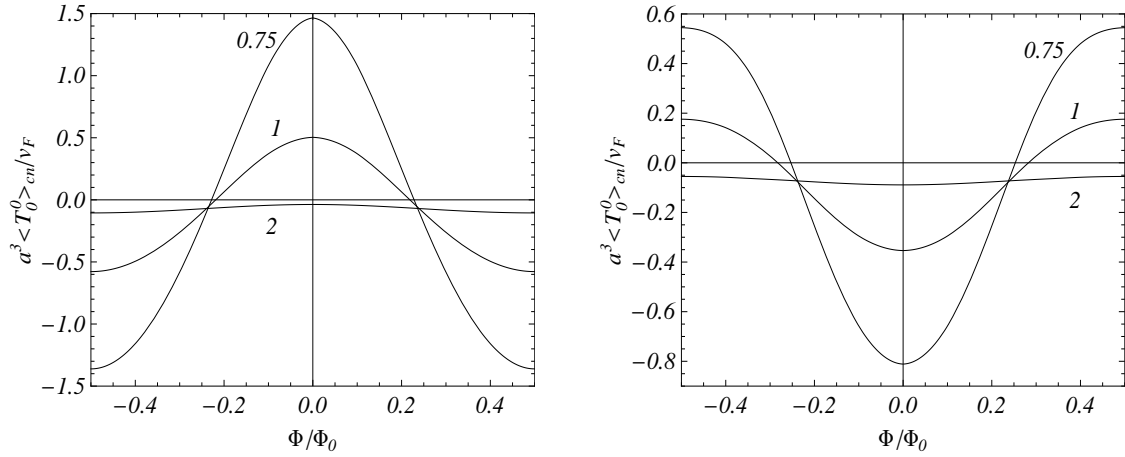


Figure 5: VEV of the energy density for metallic (left plot) and semiconducting (right plot) nanotubes, as functions of the magnetic flux in units of the flux quantum. The curves correspond to different values of the ratio  $L/a$  (labels of the curves).

## 6 Conclusions

In this paper we have considered the effect of compact spatial dimensions on the fermionic condensate and VEV of the energy-momentum tensor for a massive fermion field in the geometry of two parallel plates on which the field obeys MIT bag boundary condition. Along the compact dimensions, we have assumed periodicity conditions (2.1) with constant phases  $\alpha_l$ . The eigenvalues of the wave-vector component normal to the plates are roots of the transcendental equation (2.9). The mode sums for the fermionic condensate and the energy-momentum tensor contain series over these eigenvalues. By applying analytic continuation techniques, as the Abel-Plana-type summation formula, to these series, we have been able to explicitly extract and separate, in a cutoff independent way, the purely topological part and the contributions induced by the single plates. Purely topological contributions were investigated in Ref. [26], and here we have been mainly concerned with the boundary induced parts.

In a  $(D+1)$ -dimensional spacetime with spatial topology  $R^{p+1} \times (S^1)^q$  and with two parallel boundaries, the fermionic condensate is given by Eq. (3.23), there the first term on the rhs is a purely topological contribution and the second term is induced by the presence of the plates. The boundary induced part is always negative, whereas the purely topological one, given by Eq. (3.10), can be either positive or negative, depending on the values of the phases in the periodicity conditions along the compact dimensions. For a massless field, the general formula for the fermionic condensate could be further simplified to Eq. (3.24). Extracting there the contributions corresponding to the geometry of a single plate, the fermionic condensate could also be presented in the alternative form (3.27). The fermionic condensate induced by a single plate, located at  $z = 0$ , is given by Eq. (3.17). The condensate diverges on the boundary. For points near the boundary, the leading term in the asymptotic expansion over the distance from the plate is given by Eq. (3.20). This term does not depend on the lengths of the compact dimensions and coincides with the boundary induced contribution of the fermionic condensate for a single plate, in a space with trivial topology  $R^D$ . Far from the plate, the asymptotic behavior of the fermionic condensate essentially depends on the phases present in the periodicity conditions along the compact dimensions.

For  $\alpha_l = 0$ ,  $l = p + 2, \dots, D$ , the main contribution comes from the zero mode and the quantity  $V_q \langle \bar{\psi} \psi \rangle_{p,q}^{(1)} / N_D$  coincides with the corresponding result for a plate in topologically trivial  $(p+1)$ -dimensional space,  $R^{p+1}$ . For  $\alpha_l \neq 0$ , the zero mode is absent and the boundary induced part in the fermionic condensate is suppressed by the factor  $e^{-2m_0 z}$ , where  $m_0$  is defined in Eq. (3.22). The interference part in the representation (3.27) for the fermionic condensate is given by Eqs. (3.28) and (3.29) for massive and for massless fields, respectively. Surface divergences are contained in the single plate parts and the interference contribution is finite and positive everywhere.

The VEV of the energy-momentum tensor was investigated in Sec. 4. In the region between the plates, this VEV is given by Eq. (4.17), where the second term on the rhs is induced by the plates. The vacuum stresses along the uncompactified dimensions parallel to the plates are equal to the energy density. The boundary induced contribution to the energy density and stresses along the compact dimensions are always negative, whereas the corresponding contribution to the stress normal to the plates is positive and, moreover, a uniform function. For a massive field, the energy density and stresses along the directions parallel to the plates depend on the distance from the plate and diverge on the boundaries. For a massless field the VEV of the energy-momentum tensor is uniform, and given by Eq. (4.22). An alternative representation for the VEV of the energy-momentum tensor is (4.24), with the interference part defined in Eq. (4.25). The single plate contributions, in this decomposition, are given by (4.12). The surface divergences in the VEVs are contained in the single plate parts and the interference part is finite everywhere. Near

the plates, the VEV of the energy-momentum tensor is dominated by the single plate parts and the leading term in the corresponding asymptotic expansion is given by Eq. (4.15). In the geometry of a single plate and at large distances from the plate, compared to the length of the compact dimension, the behavior of the VEV is essentially different and crucially depends on the phases  $\alpha_l$  included in the periodicity conditions. Thus, for periodic boundary conditions,  $\alpha_l = 0$ , the dominant contribution comes from the zero mode and for the components along the uncompactified dimensions one has (no summation over  $\mu$ )  $\langle T_\mu^\mu \rangle^{(1)} \approx N_D \langle T_\mu^\mu \rangle_{R^{p+1}}^{(1)} / (V_q N_{p+1})$ ,  $\mu = 0, \dots, p+1$ , where  $\langle T_\mu^\nu \rangle_{R^{p+1}}^{(1)}$  is the corresponding VEV for plates in the space  $R^{p+1}$ . The stress along the  $l$ -th compact dimension is suppressed by the factor  $e^{-2z/L_l}$ . For  $\alpha_l \neq 0$  all components of the vacuum energy-momentum tensor are suppressed by the factor  $e^{-2m_0 z}$ .

The formulas derived for the fermionic condensate and for the VEV of the energy-momentum tensor are easily generalized to the case when a constant gauge field is present. In spite of the fact that the corresponding magnetic field strength vanishes, the non-trivial topology of the configuration leads to an Aharonov-Bohm-type effect on the vacuum expectation values. The corresponding formulas are obtained from those in the absence of a gauge field by the replacement (2.12).

The vacuum force per unit surface of the plates is determined by the normal stress and, for the region between the plates, it is given by Eq. (4.28), where the first term is the pure topological part and the second one the interaction part of the force. When the quantum field lives in all regions of space, the pure topological parts of the force acting from the left- and from the right-hand sides of every plate compensate each other, and the resulting force is just determined by the interaction part. This turns out to be always attractive, with independence of the periodicity conditions along the compact dimensions and the value of the gauge potential. In more physical situations, however, when the quantum field is confined in the region between the plates, the pure topological part contributes to the resulting force as well and in these cases the final forces can be either attractive or repulsive. Remarkably, the Casimir effect can then be used as a stabilization mechanism for both the interplate distance and for the size of the compact subspace in Kaluza-Klein-type models and in braneworld theories.

For massless fermionic fields, the Casimir densities for the two-plate geometry in conformally-flat spacetimes with compact spatial dimensions are obtained from the results above simply by using standard conformal transformation techniques. The corresponding fermionic condensate and the VEV of the energy-momentum tensor are thus given by Eq. (4.31), where the separate contributions: the one induced by non-trivial topology and the other by the boundary conditions, are given by the second terms on the right-hand sides. The most important examples of configurations of this type are dS and AdS spacetimes.

In Sect. 5, we have applied our general results to the electrons in finite-length graphene nanotubes. The long-wavelength excitations of this system is basically described by Dirac's theory, with the Fermi velocity playing the role of speed of light. The corresponding expressions for the fermionic condensate and for the Casimir densities are obtained from the results of the preceding sections by summing the contributions of the two triangular sublattices of the honeycomb lattice of the graphene sheet, with opposite signs of the phases along the compact dimension. In the presence of a magnetic flux, the fermion condensate is given by Eqs. (5.3) and (5.5), for massive and for massless fields, respectively. The pure topological contribution is then given by (5.2). In these formulas, the values  $\alpha = 0$  and  $\alpha = 1/3$  correspond to metallic and to semiconducting nanotubes, respectively. The corresponding expressions for the VEV of the energy-momentum tensor have the form (5.8) and (5.10). The VEVs are periodic functions of the magnetic flux with period equal to the flux quantum. In the absence of magnetic flux, the Casimir forces acting on the edges of the nanotube are always attractive for metallic nanotubes.

However, for semiconductor nanotubes the forces are attractive for short tubes and repulsive for longer ones. In the presence of the magnetic flux, the sign of the force for long tubes can be controlled by tuning the flux. This possibility opens the way to the design of efficient actuators driven by the Casimir force at the nanoscale, what is a most cherished goal of present day technology.

## Acknowledgments

A.A.S. was supported by the ESF Programme “New Trends and Applications of the Casimir Effect”. E.E. and S.D.O. were partially funded by MICINN (Spain) project FIS2006-02842, by CPAN Consolider Ingenio Project, and by AGAUR (Catalonia) 2009SGR-994.

## References

- [1] A. Linde, JCAP **0410**, 004 (2004).
- [2] R. Saito, G. Dresselhaus, and M. S. Dresselhaus, *Physical Properties of Carbon Nanotubes* (Imperial College Press, London, 1998); C. Dupas, P. Houdy, and M. Lahmani (Editors), *Nanoscience: Nanotechnologies and Nanophysics* (Springer, Berlin, 2007).
- [3] G.W. Semenoff, Phys. Rev. Lett. **53**, 2449 (1984).
- [4] D.P. Di Vincenzo and E.J. Mele, Phys. Rev. B **29**, 1685 (1984); J. González, F. Guinea, and M.A.H. Vozmediano, Nucl. Phys. B **406**, 771 (1993); Phys. Rev. B **63**, 134421 (2001); H.-W. Lee and D.S. Novikov, Phys. Rev. B **68**, 155402 (2003); S.G. Sharapov, V.P. Gusynin, and H. Beck, Phys. Rev. B **69**, 075104 (2004); K.S. Novoselov et al, Nature **438**, 197 (2005); D. S. Novikov and L. S. Levitov, Phys. Rev. Lett. **96**, 036402 (2006); E. Perfetto, J. González, F. Guinea, S. Bellucci, and P. Onorato, Phys. Rev. B **76**, 125430 (2007); V.P. Gusynin, S.G. Sharapov, and J.P. Carbotte, Int. J. Mod. Phys. B **21**, 4611 (2007); A.H. Castro Neto, F. Guinea, N.M.R. Peres, K.S. Novoselov, and A.K. Geim, Rev. Mod. Phys. **81**, 109 (2009).
- [5] E. Elizalde, S.D. Odintsov, A. Romeo, A.A. Bytsenko and S. Zerbini, *Zeta regularization techniques with applications* (World Scientific, Singapore, 1994); E. Elizalde, *Ten physical applications of spectral zeta functions*, Lecture Notes in Physics (Springer-Verlag, Berlin, 1995); V.M. Mostepanenko and N.N. Trunov, *The Casimir Effect and Its Applications* (Clarendon, Oxford, 1997); M. Bordag, U. Mohideen, and V.M. Mostepanenko, Phys. Rep. **353**, 1 (2001); K.A. Milton, *The Casimir Effect: Physical Manifestation of Zero-Point Energy* (World Scientific, Singapore, 2002); M. Bordag, G.L. Klimchitskaya, U. Mohideen, and V.M. Mostepanenko, *Advances in the Casimir Effect* (Oxford University Press, Oxford, 2009); M.J. Duff, B.E.W. Nilsson, and C.N. Pope, Phys. Rep. **130**, 1 (1986); A.A. Bytsenko, G. Cognola, L. Vanzo, and S. Zerbini, Phys. Rep. **266**, 1 (1996).
- [6] I.L. Buchbinder and S.D. Odintsov, Fortsch. Phys. **37**, 225 (1989).
- [7] E. Elizalde, Phys. Lett. B **516**, 143 (2001); C.L. Gardner, Phys. Lett. B **524**, 21 (2002); K.A. Milton, Grav. Cosmol. **9**, 66 (2003); E. Elizalde, J. Phys. A **39**, 6299 (2006); B. Green and J. Levin, J. High Energy Phys. **11**, 096 (2007); P. Burikham, A. Chatrabhuti, P. Patcharamaneepakorn, and K. Pimsamarn, J. High Energy Phys. **07**, 013 (2008).
- [8] V.M. Mostepanenko and I.Yu. Sokolov, Phys. Lett. A **125**, 405 (1987); J. C. Long, H. W. Chan and J. C. Price, Nucl. Phys. B **539**, 23 (1999); R.S. Decca, D. López, E. Fischbach,

- G.L. Klimchitskaya, D.E. Krause, and V.M. Mostepanenko, *Phys. Rev. D* **75**, 077101 (2007); G.L. Klimchitskaya, U. Mohidden, and V.M. Mostepanenko, *Rev. Mod. Phys.* **81**, 1827 (2009).
- [9] H.B. Cheng, *Phys. Lett. B* **643**, 311 (2006); H.B. Cheng, *Phys. Lett. B* **668**, 72 (2008); S.A. Fulling and K. Kirsten, *Phys. Lett. B* **671**, 179 (2009); K. Kirsten and S.A. Fulling, *Phys. Rev. D* **79**, 065019 (2009); E. Elizalde, S.D. Odintsov, and A.A. Saharian, *Phys. Rev. D* **79**, 065023 (2009); L.P. Teo, *Phys. Lett. B* **672**, 190 (2009); L.P. Teo, *Nucl. Phys. B* **819**, 431 (2009); L.P. Teo, *JHEP* **0906**, 076 (2009); L.P. Teo, *JHEP* **0911**, 095 (2009).
- [10] K. Poppenhaeger, S. Hossenfelder, S. Hofmann, and M. Bleicher, *Phys. Lett. B* **582**, 1 (2004); A. Edery and V.N. Marachevsky, *Phys. Rev. D* **78**, 025021 (2008); A. Edery and V.N. Marachevsky, *JHEP* **0812**, 035 (2008); F. Pascoal, L.F.A. Oliveira, F.S.S. Rosa, and C. Farina, *Braz. J. Phys.* **38**, 581 (2008); L. Perivolaropoulos, *Phys. Rev. D* **77**, 107301 (2008).
- [11] V.A. Rubakov, *Phys. Usp.* **44**, 871 (2001); P. Brax and C. Van de Bruck, *Classical Quantum Gravity* **20**, R201 (2003); R. Maartens, *Living Rev. Relativity* **7**, 7 (2004).
- [12] L. Randall and R. Sundrum, *Phys. Rev. Lett.* **83**, 3370 (1999).
- [13] W. Goldberger and I. Rothstein, *Phys. Lett. B* **491**, 339 (2000); S. Nojiri, S.D. Odintsov, and S. Zerbini, *Classical Quantum Gravity* **17**, 4855 (2000); A. Flachi and D. J. Toms, *Nucl. Phys. B* **610**, 144 (2001); J. Garriga, O. Pujolàs, and T. Tanaka, *Nucl. Phys. B* **605**, 192 (2001); E. Elizalde, S. Nojiri, S.D. Odintsov, and S. Ogushi, *Phys. Rev. D* **67**, 063515 (2003); A.A. Saharian and M.R. Setare, *Phys. Lett. B* **584**, 306 (2004); A. Flachi, A. Knapman, W. Naylor, and M. Sasaki, *Phys. Rev. D* **70**, 124011 (2004); M. Frank, I. Turan, and L. Ziegler, *Phys. Rev. D* **76**, 015008 (2007); L.P. Teo, *Phys. Lett. B* **682**, 259 (2009); A. Flachi and T. Tanaka, *Phys. Rev. D* **80**, 124022 (2009); L.P. Teo, *Phys. Rev. D* **82**, 027902 (2010); L.P. Teo, *JHEP* **1010**, 019 (2010).
- [14] A. Knapman and D. J. Toms, *Phys. Rev. D* **69**, 044023 (2004); A. A. Saharian, *Nucl. Phys. B* **712**, 196 (2005).
- [15] A. Flachi, J. Garriga, O. Pujolàs, and T. Tanaka, *J. High Energy Phys.* **0308**, 053 (2003); A. Flachi and O. Pujolàs, *Phys. Rev. D* **68**, 025023 (2003); A.A. Saharian, *Phys. Rev. D* **73**, 044012 (2006); A.A. Saharian, *Phys. Rev. D* **73**, 064019 (2006); A.A. Saharian, *Phys. Rev. D* **74**, 124009 (2006); R. Linares, H.A. Morales-Técotl, and O. Pedraza, *Phys. Rev. D* **77**, 066012 (2008); M. Frank, N. Saad, and I. Turan, *Phys. Rev. D* **78**, 055014 (2008).
- [16] S. Bellucci and A.A. Saharian, *Phys. Rev. D* **80**, 105003 (2009).
- [17] T. Inagaki, T. Muta, and S.D. Odintsov, *Prog. Theor. Phys. Suppl.* **127**, 93 (1997).
- [18] A. Flachi and T. Tanaka, arXiv:1012.0463.
- [19] K. Johnson, *Acta Phys. Polonica B* **6**, 865 (1975).
- [20] S. G. Mamaev and N. N. Trunov, *Sov. Phys.* **23**, 551 (1980).
- [21] R. D. M. De Paola, R. B. Rodrigues, and N. F. Svaiter, *Mod. Phys. Lett. A* **14**, 2353 (1999).
- [22] E. Elizalde, F.C. Santos, and A.C. Tort, *Int. J. Mod. Phys. A* **18**, 1761 (2003).

- [23] C.A. Lütken and F. Ravndal, *J. Phys. G* **10**, 123 (1984); S.A. Gundersen and F. Ravndal, *Ann. Phys.* **182**, 90 (1988).
- [24] P. Sundberg and R.L. Jaffe, *Ann. Phys.* **309**, 442 (2004).
- [25] C.D. Fosco and E.L. Losada, *Phys. Rev. D* **78**, 025017 (2008).
- [26] S. Bellucci and A.A. Saharian, *Phys. Rev. D* **79**, 085019 (2009).
- [27] S. Bellucci, A.A. Saharian, and V.M. Bardeghyan, *Phys. Rev. D* **82**, 065011 (2010).
- [28] N.D. Birrell and P.C.W. Davis, *Quantum Fields in Curved Space* (Cambridge University Press, Cambridge, England, 1982).
- [29] A. Romeo and A. A. Saharian, *J. Phys. A: Math. Gen.* **35**, 1297 (2002).
- [30] A. A. Saharian, *The Generalized Abel-Plana Formula with Applications to Bessel Functions and Casimir Effect* (Yerevan State University Publishing House, Yerevan, 2008); Preprint ICTP/2007/082; arXiv:0708.1187.
- [31] A.A. Saharian, *Class. Quantum Grav.* **25**, 165012 (2008); E.R. Bezerra de Mello and A.A. Saharian, *J. High Energy Phys.* **12** (2008) 081.
- [32] A.A. Saharian, *Phys. Rev. D* **69**, 085005 (2004).
- [33] V. P. Gusynin, V. A. Miransky, and I. A. Shovkovy, *Phys. Rev. D* **52**, 4718 (1995).
- [34] C. Chamon, *Phys. Rev. B* **62**, 2806 (2000); C.-Y. Hou, C. Chamon, and C. Mudry, *Phys. Rev. Lett.* **98**, 186809 (2007).
- [35] G. Giovannetti, P.A. Khomyakov, G. Brocks, P.J. Kelly, and J. van den Brink, *Phys. Rev. B* **76**, 073103 (2007); S.Y. Zhou et al., *Nature Mater.* **6**, 770 (2007).
- [36] G.W. Semenoff, V. Semenoff, and F. Zhou, *Phys. Rev. Lett.* **101**, 087204 (2008).
- [37] M. Bordag, B. Geyer, G.L. Klimchitskaya, and V.M. Mostepanenko, *Phys. Rev. B* **74**, 205431 (2006); M. Bordag, I.V. Fialkovsky, D.M. Gitman, and D.V. Vassilevich, *Phys. Rev. B* **80**, 245406 (2009); M. Bordag, I.V. Fialkovsky, D.M. Gitman, and D.V. Vassilevich, arXiv:1003.3380; D. Drosdoff and L.M. Woods, arXiv:1007.1231; B.E. Sernelius, arXiv:1011.2363.
- [38] Yu.V. Churkin, A.B. Fedortsov, G.L. Klimchitskaya, and V.A. Yurova, *Phys. Rev. B* **82**, 165433 (2010).
- [39] H. Ajiki and T. Ando, *J. Phys. Soc. Jpn.* **62**, 1255 (1993); *Physica B* **201**, 349 (1994); A. Bachtold et al., *Nature* **397**, 673 (1999); S. Zaric et al., *Science* **304**, 1129 (2004); U.S. Coskun et al., *Science* **304**, 1132 (2004); J. Cao, Q. Wang, M. Rolandi, and H. Dai, *Phys. Rev. Lett.* **93**, 216803 (2004); B. Lassagne et al., *Phys. Rev. Lett.* **98**, 176802 (2007); M.-G. Kang et al., *Phys. Rev. B* **77**, 113408 (2008).
- [40] E.R. Bezerra de Mello, V.B. Bezerra, A.A. Saharian, and V.M. Bardeghyan, *Phys. Rev. D* **82**, 085033 (2010); S. Bellucci, E.R. Bezerra de Mello, A.A. Saharian, arXiv:1101.4130.